Passive Motion Control of Super Tall Buildings: Tuned Mass and Viscous Dampers in Taipei 101

by

Zheng Li Gong

B.S. in Civil and Environmental Engineering
Massachusetts Institute of Technology, 2008

Submitted to the Department of Civil and Environmental Engineering
In Partial Fulfillment of the Requirements for the Degree of
Master of Engineering in Civil and Environmental Engineering

at the

Massachusetts Institute of Technology
June 2009

Signature of Author: _____

Department of Civil and Environmental Engineering
May 19, 2009

Certified by: _____

Jerome J. Connor
Professor of Civil and Environmental Engineering
Thesis Supervisor

Accepted by: _____

Daniele Veneziano
Chairman, Departmental Committee for Graduate Students

Passive Motion Control of Super Tall Buildings:
Tuned Mass and Viscous Dampers in Taipei 101

by

Zheng Li Gong

Submitted to the Department of Civil and Environmental Engineering
On May 19 2009 in Partial Fulfillment of the Requirements for the Degree of
Master of Engineering in Civil and Environmental Engineering

Abstract

As tall buildings keep becoming taller, they become more susceptible to dynamic excitations such as wind and seismic excitations. One way to reduce structural vibration under dynamic excitations is by placing damping devices in the buildings. In this thesis, the design concept, design procedure and some current applications of tuned mass and viscous dampers are discussed. Taipei101 was used as an example to compare the performance of the two damping schemes. It was modeled in a two-dimensional scheme in SAP2000 and a TMD was placed on its top to study its effect on the structural response due to wind and seismic excitations and confirm with the actual results. A sensitivity study was then performed to study the effect of varying the mass ratio on the structural response. A second TMD was then placed at the location where the maximum deflection occurs for the second mode to evaluate its effectiveness in reducing structural response. Finally, twelve viscous dampers were placed in the model to study their effects on the structural response. Time-history and steady-state analysis in SAP2000 were used for the wind and seismic analyses.

Thesis Supervisor: Jerome J. Connor

Title: Professor, Civil and Environmental Engineering

Acknowledgements

My first and most earnest acknowledgement must go to my advisor, Professor Jerome Connor. He contributed tremendously to my development, academically, professionally and personally. He was always there with so much knowledge, encouragement, and patience.

I would also like to acknowledge my parents, who have always been encouraging and supporting me to pursue a higher education. To me, my mother has always been the brightest and the most diligent woman in the world. I will always follow her spirit in my future professional and personal life. To me, my father has always been the most loving and understanding father I can imagine having. Dad, thanks for always being there and supporting my dreams.

Table of Contents

List of Figures

List of Tables

1. Introduction

As tall buildings become taller, they also become stronger and lighter: construction using higher-strength materials, lighter-weight floors, and curtain wall systems has reduced building weight, stiffness and damping values [1]. These tall buildings become therefore more susceptible to wind loads and wind-induced excitations [2], which usually depend on various factors such as intensity of wind loads, building size, shape, and dynamic properties [3]. Furthermore, some of the tall buildings located in active seismic regions are susceptible to seismic events as well.

The conventional way is to increase the effective stiffness of the building to keep it in elastic or near elastic range. This is effective in increasing the structural strength, but not always effective in reducing the structural motion under dynamic excitations, which is one major design issue especially for super tall buildings. In fact, designing buildings to behave elastically or near the elastic range during strong dynamic excitations is not economical, and in many cases is not feasible. Therefore, enabling the building to dissipate energy by means of mechanical devices may be more attractive. One way to achieve that goal is to install damping systems to alleviate the impact of dynamic excitations to a building and thus control the building vibration. The selection of a vibration control device is based on several factors, including efficiency, compactness, weight, material and operating cost, maintenance requirements and safety [4].

Among the various damping methods which have been studied, the tuned mass damper (TMD) and viscous damper systems have been widely used [5]. TMDs are auxiliary damping devices attached to the top of a building in order to increase the effective damping and decrease the building vibrations under wind loads and wind-induced excitations [6]. Viscous dampers have

been used to mitigate the building vibrations under not only wind loads and wind-induced excitations but also seismic-induced excitations for tall buildings located in high wind and active seismic regions.

The goal of this thesis is to study and compare the use of tuned mass and viscous dampers in super tall buildings. The second and third chapters compare the concepts, design procedures and current applications of the two. Chapter four presents a design summary of a super tall building Taipei101, including a description of its TMD system and the effectiveness of the TMD in reducing the building response due to wind and seismic-induced excitations. Taipei101 is chosen because it is one of those tall buildings susceptible to both wind and seismic loads. Although there have been several studies published by the designer and has been studied in a number of research studies, there has been little done to show the seismic viability of the design. In chapter five, a simplified two-dimensional model is created for Taipei101 to represent its basic structural system. The purpose is to verify the model by comparing its performance under wind and seismic excitations with the values obtained from literature review. In chapter six, a TMD is placed on top of the building to verify its effectiveness under wind excitations and to investigate its effectiveness under seismic excitations. Then a number of viscous dampers are placed to investigate their effectiveness under wind and seismic excitations. Several parametric studies are performed to determine the optimal number and locations of each type of damping system.

2. Tuned Mass Damper Systems

2.1 Introduction

A tuned mass damper (TMD) is a device which consists of a mass, a spring and a damper. It is commonly attached to a primary system and is an effective and reliable way to control structural vibration and reduce the dynamic response induced by wind and seismic loads. The effectiveness of a TMD under narrow-band and wide-band excitations has been investigated. It was found that the narrower the excitation frequency band width, the more effective the TMD is [6]. TMD is designed such that its natural frequency is tuned in resonance with a particular frequency (often the fundamental frequency) of the primary structure, so that when that frequency is excited, the TMD will resonate out of phase with the structure. The energy caused by vibration is transferred from the primary structure to the TMD and is dissipated by the damping from the TMD [7] [8].

Figure 1a shows a typical configuration of a TMD: mass m_2 is connected to the main structure with mass m_1 with a spring k_2 and a dashpot c_2. The main structure has an intrinsic damping of c_1 and stiffness k_1. The effectiveness of a TMD can be evaluated in terms of an effective damping by replacing the two-degree-of-freedom system with an equivalent one-degree-of-freedom system shown in Figure 1b. Once the effective damping C_e and the external excitation is defined, the relative movement of a TMD can be determined. The effectiveness of a TMD on a one-degree-of-freedom system can be extended to a continuous system with a modal approach [4].

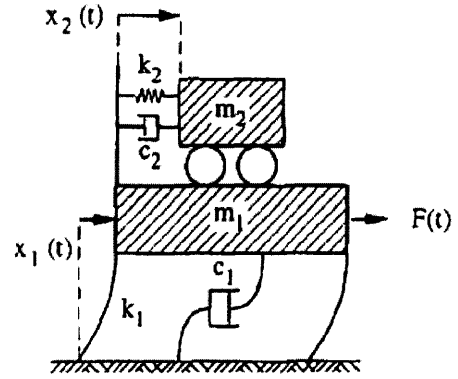

(a)

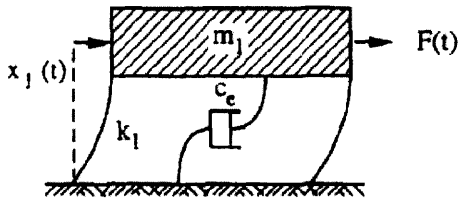

(b)

Figure 1: A typical TMD configuration (4)

Despite the advantages of the TMD system, it is not always the best solution for the following reasons [9]:

1. TMDs are effective only for the particular mode they are tuned for. For structures with more than one mode of concern, one TMD would not be sufficient.
2. TMDs usually take a significant amount of rental space.
3. The period of a structure may change over time. TMDs may become less effective and they are not as easily adjusted.
4. TMDs are not as effective for seismic events with wide-band excitations.

2.2 Design procedure

A simple illustration of the preliminary design of a TMD for a single-degree-of-freedom system shown in Figure 2 was given by Connor [8]. The design of a TMD includes the specification of the damper mass, the damper stiffness, and the damping coefficient. A near-optimal approximation for the frequency of the damper given by Connor is shown below.

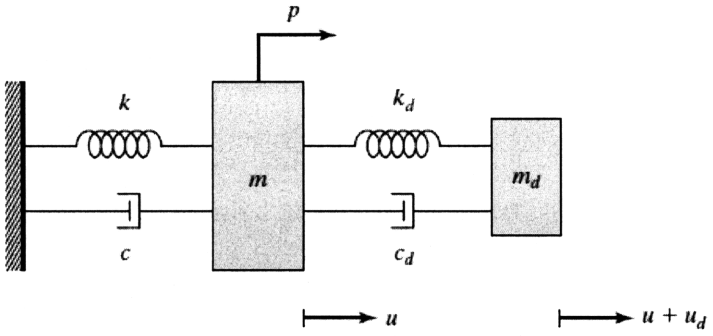

Figure 2: A single-degree-of freedom TMD system (8)

Known:

Effective damping $\xi_e = \frac{\bar{m}}{2}\sqrt{1+\left(\frac{2\xi}{\bar{m}}+\frac{1}{2\xi_d}\right)^2}$

Allowable displacement $\widehat{u_d} = \frac{1}{2\xi_d}\,\hat{u}$

Make $\xi = 0$, $\xi_e = \frac{\bar{m}}{2}\sqrt{1+\left(\frac{\hat{u}_d}{\hat{u}}\right)^2}$

Usually, $\hat{u}_d$ is taken to be an order of magnitude greater than $\hat{u}$. Therefore,

$$\frac{\bar{m}}{2}\sqrt{\left(\frac{\hat{u}_d}{\hat{u}}\right)^2} \approx \xi_e$$

$$\bar{m} = 2\xi_e\left(\frac{1}{\hat{u}_d/\hat{u}}\right)$$

$$\xi_d = \frac{1}{2}\left(\frac{\hat{u}}{\hat{u}_d}\right)$$

$$k_d = mk$$

Parametric studies are often used to assess the performance of a TMD system in buildings. Xu et al.[10] [11] and Kim, You, and Kim [6] studied the effectiveness of TMD in reducing the structural response to wind-induced along-wind and crosswind. It was generally agreed that while TMDs are effective in reducing the particular modes of vibration being controlled, the higher modes of the structures are often not affected. Separate TMDs will be required if the higher modes become dominant [4]. Kim et al. observed a general decrease in building excitations with a TMD, concluding that TMD was more effective when the inherent damping ratio of the building was very low, and for the same inherent damping ratio of the building, TMD was more effective when it had a higher mass ratio [6].

2.3 Current applications

TMD systems have been successfully placed in a number of tall buildings worldwide, in addition to Taipei101 which will be discussed in later chapters. Four applications of TMD system are presented below.

Citicorp Center: 1 TMD tuned to the first mode

A tuned mass damper was installed on the 63rd floor, the crown of the 279m building with a fundamental period of 6.5 seconds and an inherent damping of 1%. The TMD consists of a 400-ton concrete block bearing on a thin film of oil [12]. The system is automatically activated when

the horizontal acceleration exceed 0.003g for two consecutive cycles and is automatically deactivated when the acceleration does not exceed 0.00075g in either axis over a 30-minute interval. This system cost around 1.5 million dollars, and was expected to reduce the sway of the structure by 50%. Citicorp Tower was the first skyscraper to feature a TMD in the U.S. [8].

John Hancock Tower: 2 TMDs tuned to the first mode

Two tuned mass dampers were installed on the 58th story of the 60-story John Hancock Tower to reduce the response to wind gust loading. The two 2700kN dampers consisting of two steel boxes filled with lead were installed at two opposite ends of the floor to counteract sway and twisting of the structure. The system is automatically activated when the horizontal acceleration exceed 0.003g for two consecutive cycles. This system cost around 3 million dollars, and was expected to reduce the sway of the structure by 40 to 50% [8].

Canadian National Tower: 2 TMDs tuned to the second and fourth modes

Two tuned mass dampers were installed for the antenna mast on top of the Canadian National Tower in Toronto. The two dampers, located at 488 meter and 503 meters of the 553 meter high tower, are two doughnut-shaped steel ring filed with lead. The dampers are tuned to the second and fourth modes of vibration to reduce antenna bending loads. The frequency of the first bending mode (the third mode) is 0.775 Hz, approximately 1.3 seconds. The first and third modes did not require additional damping [Connor]. The natural frequency of the TMDs was 0.727 Hz, and the damping ratio was 0.142 [8].

Crystal Tower: 1 pendulum-type TMD tuned to the first and second modes

A pendulum-type TMD was installed for the Crystal Tower in Osaka, Japan to decrease the wind induced motion in north-south direction and east-west direction. Six air cooling and heating ice thermal storage tanks (540 tons in total) were hung as pendulums. Four of them (360 tons) with a pendulum length of 4 meter were to slide in the north-south direction, while the other two (180 tons) with a pendulum length of 3 meter were to slide in the east-west direction. This system cost around $350,000 dollars, and was expected to reduce the sway of the structure by 50% [8].

	Citicorp	**John Hancock**	**CN**	**Crystal**
	279m	60-story	553m	157m
No. dampers	1	2	2	6
Weight/damper	400 tons	270 tons	4.6 tons	90 tons
Material	concrete	lead	lead	ice
Reduction in sway	50%	40-50%	80%	50%
Acceleration	0.003g	0.003g		
Cost	$1.5 million	$3 million		$350,000

Table 1: A list of 4 current applications of TMD

3. Viscous Damper Systems

3.1 Introduction

An alternative damping system for tall buildings is fluid viscous damper. Viscous damping can be defined as the energy dissipation mechanism where the damping force is a function of the relative velocity measure and the damping coefficient [8]. Along with visco-elastic dampers and friction dampers, fluid viscous dampers operate based on the relative motion between two certain points in the structure. They are piston-type devices which generate a resistance force when the fluid inside passes through. Figure 3 shows an example of a seismic viscous damper with 50,000 pounds output manufactured by Taylor Device Inc. Figure 4 shows the different components in a typical viscous damper.

Figure 3: A seismic viscous damper by Taylor Device Inc. [8]

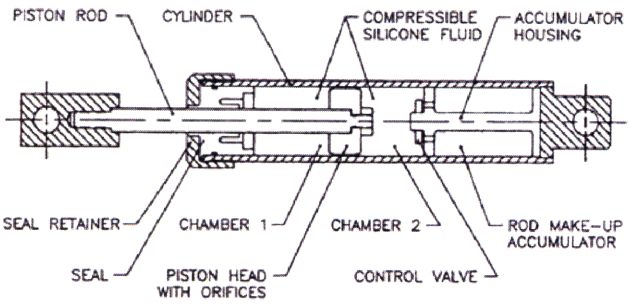

Figure 4: Different components in a viscous damper [15]

In addition to be used for new building design, viscous dampers always seem more appropriate for rehabilitation of existing structures. The main advantage is that the forces viscous dampers generate are out of phase with the forces in the structural columns due to displacements. Therefore, they do not usually require column and foundation strengthening [13] [14]. Compared to TMDs, viscous dampers have the following advantages:

1. Viscous dampers do not need to be tuned to a particular mode (i.e. frequency). They work for a range of frequencies.
2. Viscous dampers are much smaller in size and can be located at multiple locations.
3. Viscous dampers can be more easily replaced or relocated.
4. Viscous dampers are more effective for seismic events than TMDs because they work for a range of frequencies.

Viscous dampers are often compared with base isolation, because they share the same objective of significantly decreasing the response of a structure under seismic excitations. Base isolation is usually elastomeric pads or sliding bearing at the bottom of a structure, connecting it to the foundation. It reduces structural excitation through decoupling the structure from the ground, greatly increasing the natural period of the structure. The main disadvantage of base isolation is that it requires the entire structure to be cut loose and physically separated from the foundation. This means all the vertical load bearing columns have to be cut to provide an approximately 18 inch gap between the structure and the foundation in order to insert the isolation pads or bearing. The actual construction is often involved with adding a large number of braced frames or concrete shear walls [15].

Viscous dampers are also used to reduce the structural response under seismic excitation, but with adding damping to a structure to significantly reduce its resonant response to a seismic event. The added damping does not significantly alter the natural period of the structure, but increases the effective damping to a much higher level.

Figure 5a shows one typical configuration of viscous dampers, in which case it is incorporated into the diagonal element between two stories. This configuration can be used for new structure as well as existing structures. Figure 5b shows another configuration, in which it connects the apex of a chevron brace to the adjacent beams. Two dampers are connected to each apex, one in compression and the other in tension.

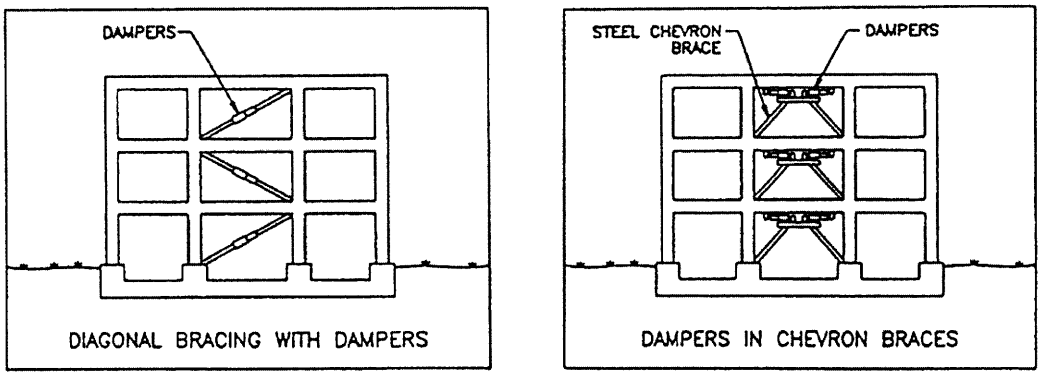

Figure 5: Two typical locations to place viscous dampers (15)

3.2 Design procedure

The damping force is a function of the damping coefficient and the relative velocity between the two ends of the damper, given by

$$F = c\,\dot{u}$$

Where c is the damping coefficient, a property of the damping device, and $\dot{u}$ is the velocity. The work W done on the damping device under a periodic excitation

$$u = \hat{u}sin\Omega t$$

during a interval from t1 to t2 is given by

$$W = \int_{t1}^{t2} F\dot{u}dt$$

The work done for one full cycle is therefore

$$W = c\pi\Omega\hat{u}^2$$

The optimal design of viscous damping has been proposed by several researchers, often through a series of parametric studies in term of the optimal size and location to install viscous dampers. Constantinou and Tadjbakhsh derived an optimal damping coefficient for a viscous damper installed on the first storey of a building [16]. Fu and Kasai estimated the damping needed and compared the use of viscous and viscoelastic dampers [17]. Lavan and Levy studied the optimization problem of minimizing the added damping of prelocated dampers subject to a constraint on the maximum inter-storey drift for a frame excited by a series of ground motion records [13].

4. Taipei101: Design Summary

Located in Xinyi District in Taipei, Taiwan, Taipei 101 is currently the world's tallest completed skyscraper. It has 101 floors above the ground and 5 floors underground, with a total height of 508 meters from ground to top. Its name reflects its location in Taipei's business district and its total floor count.

The most significant feature of Taipei101 is the number eight used in the design, which was a symbol for good luck in Chinese culture. The structure has 8 canted sections, each of which has 8 floors, as well as 8 super-columns, 16 core columns, and 8-meter-long Chinese Ru-yi symbols which are placed on 4 sides of the building.

The total rentable space of Taipei 101 is 1.8 million square feet. The first 3 floors are the main lobby. Floor 9 to 34 is the low zone. On floor 35 and 36, there is a sky lobby. Floor 35-58 is the mid zone. On 59 and 60, there is another sky lobby. Then floor 59 to 84 is the high zone. There is an observatory on the 89^{th} floor, and an observation deck on the 90^{th} floor. From floor 92 to 100 is the communication floors.

4.1 Structural system

Taipei 101 features a variety of design issues which apply to many high-rise buildings nowadays, including difficult foundation conditions, unusual building shapes, demanding lateral stiffness requirements, mixed structural materials, wind/building interaction, occupant comfort criteria, seismic demands, special ductility details and fatigue life concerns. In fact, it is more challenging

to design and construct a skyscraper in Taipei than most other locations, because of the typhoon winds, high seismic risks, and poor soil conditions [18].

The structure was first designed to meet the strength and stiffness requirements for vertical and lateral loads by base structural members. A damping system was then implemented on the top to reduce the excessive lateral motion due to wind.

4.1.1 Gravity systems

Gravity loads are carried by the core columns and the perimeter super-columns. Within the core, there are 16 columns along the 4 lines of bracing in each direction. The columns are all box sections constructed of steel plates and filled with concrete (up to the 62^{nd} floor). On the perimeter, there are 2 super-columns on each face, which are all constructed of steel box sections filled with high strength concrete (up to the 62^{nd} floor) to provide the required strength and stiffness. The whole structure is a special moment resisting frame (SMRF), a rigidly-connected grid of stiff beams and columns [19]. At each 8-story section, gravity load is transferred to the super columns through trusses.

4.1.2 Lateral systems

The lateral systems are composed of the following structural elements: braced frames in the core, outriggers, super-columns, and the moment resisting steel frame (Figure 6). Among them, the braced core and the outriggers were to carry most of the lateral forces, while the super-columns and the SMRF were to help reduce the moment induced by the lateral forces on the core. The lateral systems were sized to limit the story drift to be under h/200, which was for a wind load

with 50 year return period [19]. 11 outrigger trusses in total were installed at the 8-story sections. 6 of them are one story deep for mechanical considerations. The other 5 are two-story deep for architectural considerations.

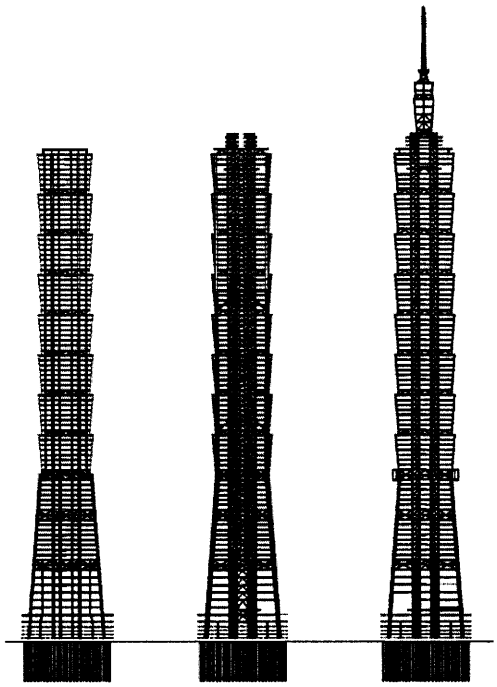

Figure 6: Lateral system (19)

4.2 Wind engineering

For tall buildings like Taipei101, wind-tunnel tests are often required. A wind tunnel test increases the accuracy of the analysis by taking into account of the aerodynamic properties of the building and its site conditions, and eventually can often result in significant savings in construction cost.

After a series of wind tunnels test by Rowan Williams Davies & Irwin Inc. (RWDI), the rectangular cross sections were modified to include double-stairstep notched corner to

dramatically reduce crosswind excitation, which resulted in a 25% reduction in design base moment [20].

4.2.1 Building TMD

The wind tunnel test results revealed that under the wind with a half year return period, the peak acceleration at the top would be 7.9 milli-g, exceeding the 5.1 milli-g design limit in Taiwan. A pendulum-type TMD was therefore installed at the top 5 floors of the structure to reduce the motion due to wind. The TMD weights 730 ton, 0.26% of the total weight of the structure, and has a length of 11.5 meters (floor 88 to 92). As the largest TMD installation to date, it was expected to reduce the acceleration at the top from7.9 milli-g to 5.0 milli-g [21].

4.2.2 Pinnacle TMDs

Due to the slenderness of the pinnacle (60 meters) on top of the structure and the windy climate in Taipei region, a number of modes of the pinnacle are excited under common wind speeds and thus cause vortex induced oscillation. The result is the rapid accumulation of fatigue cycles. TMDs are only effective in reducing structural response due to narrow banded excitations, and therefore are usually tuned to the most severe mode. However, mode 10 and 12 are both excited under the effect of vortex induced oscillation, and the frequencies (0.85Hz and 1.08Hz) associated with the two modes are too far apart to be resolved by one single TMD. Therefore, two compact 5-ton TMDs were installed, each of which was to target at a frequency.

4.3 Seismic engineering

Normally super tall buildings are less susceptible to seismic-induced excitations due to their relatively high fundamental periods. However, being located in a high seismic zone, the risk of structural damage under seismic events cannot be neglected for Taipei101. A number of site-specific seismic ground acceleration time histories for earthquakes with up to 100 year return periods were used in the seismic analysis of the Taipei101 model. Motioneering Inc. explained that for earthquakes with longer return periods, time domain position responses were used due to the non-linearity of the structural response. During time domain simulations, it was assumed conservatively that the building TMD does not reduce the response levels during these rare seismic events [21].

4.3.1 Building TMD

The building TMD is mainly used to resist narrow-band excitations such as vortex induced oscillations, and not as effective (or not effective at all) for seismic events. The reason is that the TMD is often tuned for the first mode of the structure. For wide-band excitations such as seismic events (especially the ones with long return periods), the TMD essentially remains still in an inertial reference frame. In the case of Taipei101, the primary structural response, the TMD system, would remain linear, whereas a secondary system would be in use and become nonlinear. This secondary system (the bumper system) is consisted of 8 viscous dampers, installed under the TMD. It is activated only when relative amplitudes are over 1.5 meters [21].

4.3.2 Pinnacle TMDs

Under strong-to-extreme seismic events, the two pinnacles TMDs will not be effective in reducing vibrations for a similar reason as for the building TMD. Furthermore, there will be potential risk of the collision between the TMDs and the pinnacle. The final solution was to "lock out" the TMDs with secondary mechanisms under extreme events. The TMDs will then move as a part of the pinnacle structure.

5. Taipei 101: Analysis

5.1 Basic structural system

To accurately and efficiently represent the structural system, a two-dimensional scheme was used as shown in Figure7: A continuous frame element was first created to represent the structural core (the section shaded in blue in Figure 8. It consists of a steel-braced concrete core, 16 concrete-filled steel columns up to the 62nd floor and the partial floor system close to the structural core. Two continuous frame elements were then added to both sides of the structural core to represent the structural perimeter, as shown in the section shaded in grey in Figure 8. The structural perimeter consists of 8 concrete-filled steel columns up to the 62nd floor, as well as the partial floor system close to the perimeter of the structure. Horizontal frame elements were then created to connect the super columns with the core every 8 stories. Finally, the restrains were assigned: The core is fixed to the ground, whereas the super-columns and pinned supported.

The two-dimensional "three columns" modeling scheme was chosen over a two-dimensional "one cantilever" scheme in which the structure would be modeled as a cantilever beam. The two-dimensional scheme would add some complications to the calibration of the model at the initial stage of the analysis. However, it was considered necessary because viscous dampers would be added to the outriggers later on. In addition, this scheme would allow a better understanding of the effect of TMD and viscous dampers on each section of the structure under different loadings. On the other hand, a more complicated three-dimensional scheme was considered initially, but was determined to be unnecessary for this bi-axially symmetric structure.

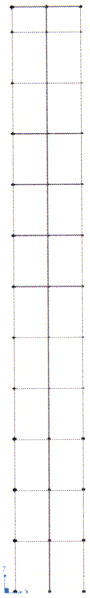

Figure 7: 2D scheme in SAP2999

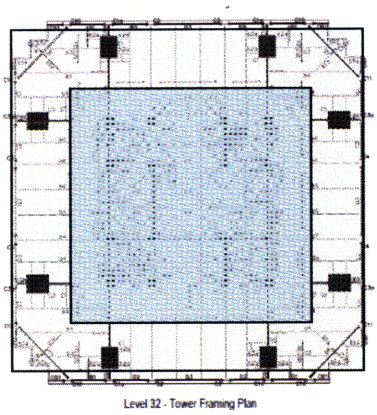

Figure 8: Taipei101 floor plan

Structural perimeter

The material and section properties of the super columns were assigned first, because the structural information of the super columns was more available. This would allow us to fix the properties of the super columns and modify other structural elements during model calibration.

Outside dimensions of the super-columns were extracted from various reports, as shown in Table 2. The cross section varies from 3.0x2.4m at its base to 2.0x1.6m at its top.

Floor	Height [m]	Super-column dimension [m]
90-101	16	2.0x1.6
82-90	33	2.0x1.6
74-82	33	2.2x1.8
66-74	33	2.4x2.0
58-66	33	2.4x2.0
50-58	33	2.6x2.2
42-50	33	3.0x2.4
34-42	33	3.0x2.4
26-34	33	3.0x2.4
0-26	100	3.0x2.4

Table 2: Outside dimensions of the super-columns

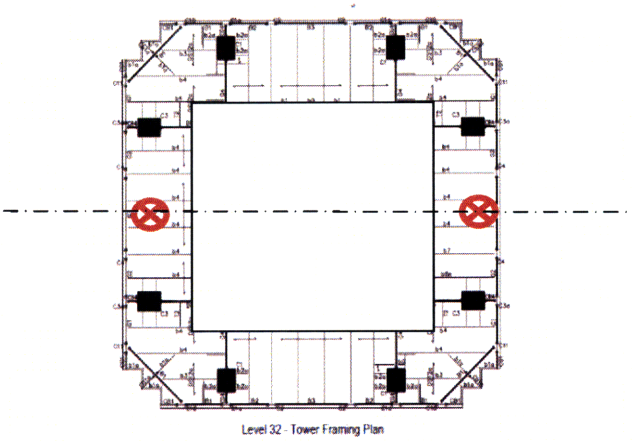

Figure 9: Perimeter system

Up to the 62nd floor, the steel super columns are filled with 10,000psi high strength concrete (shaded sections in Table 2), and stiffened with steel stiffeners, shear studs, internal cross-ties and rebars. Among these structural elements, the steel plates of a thickness of 80mm and a Young's Modulus of 200GPa and the high strength concrete fills with a Young's Modulus of 30GPa were considered in the SAP model. The moment of inertia of the 8 super columns about

the center plane, as well as the torsional constant of the 8 super columns and the floor slabs about the 2 frame elements were calculated and divided evenly to be assigned to the 2 frame elements in the SAP model. Figure 9 shows the location of the 2 "pseudo columns". A composite material property was then assigned. Finally, line masses were added to the frame elements to represent the portion of the total structural weight (assumed to be 40%, while the rest 60% is supported by the core) that the structural perimeter supports. This procedure was repeated for each 8-story section to represent the structural perimeter.

Structural core

The structural core was considered next. The dimensions of the core columns could be estimated using the structural drawings, as shown in Table 3. The cross section varies from 1.0x1.0m at its base to 1.48x1.48m at its top.

Similar to the super-columns, the steel core-columns are filled with 10,000psi high strength concrete (shaded sections in Table 3) up to the 62nd floor. The steel plates of a thickness of 80mm and a Young's Modulus of 200GPa and the high strength concrete fills with a Young's Modulus of 30GPa were considered in the SAP model. The moment of inertia of the 16 core columns about the center plane, as well as the torsional constant of the 16 core columns about the center frame element were calculated and assigned to the frame elements in the SAP model Figure 10. A composite material property was then assigned. Finally, line masses were added to the frame element to represent the portion of the total structural weight (assumed to be 60%, while the rest 40% is supported by the perimeter system) the structural core supports. This procedure was repeated for each 8-story section to most accurately represent the structural core.

Floor	Height [m]	Core-column Dimension [m]
90-101	16	1.0x1.0
82-90	33	1.0x1.0
74-82	33	1.1x1.1
66-74	33	1.3x1.3
58-66	33	1.3x1.3
50-58	33	1.3x1.3
42-50	33	1.48x1.48
34-42	33	1.48x1.48
26-34	33	1.48x1.48
0-26	100	1.48x1.48

Table 3: Outside dimensions of the structural core

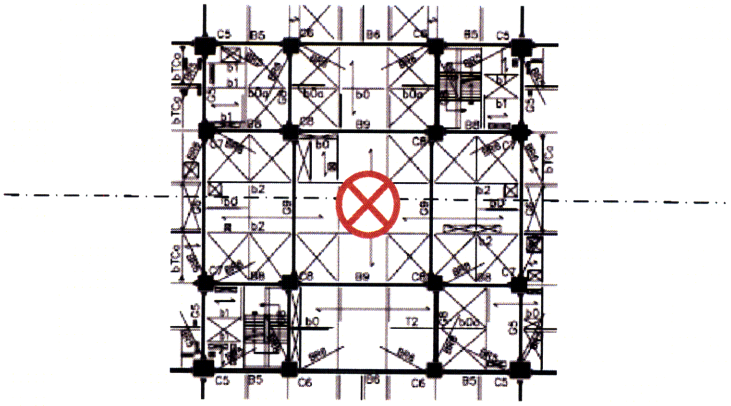

Figure 10: Structural core

Outriggers

Since not enough structural information was available for modeling the outriggers, the dimensions and section properties were to be modified for calibration purposes in order to achieve the desired fundamental period of the actual structure. Steel elements of various dimensions and stiffnesses were assigned to the outriggers to connect the core frame element with the two column frame elements (Figure 11).

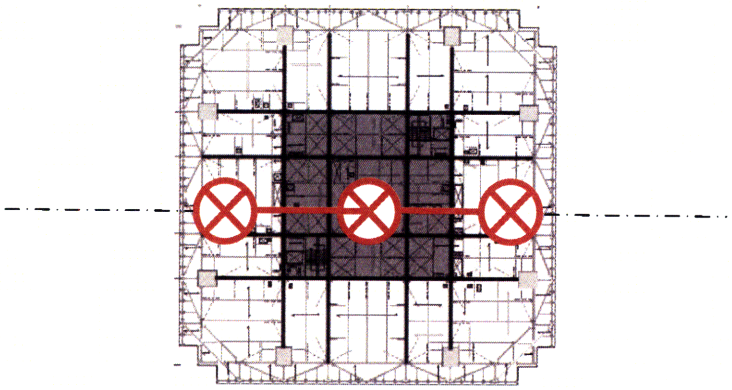

Figure 11: Outriggers

After all structural elements were initially specified, a few iterations were performed and the outriggers were modified in order to achieve the fundamental period of 6.8 seconds.

5.2 Modal analysis

The mode shapes and the corresponding periods of the first 10 modes were obtained. The first 4 mode shapes are shown in Figure 12. Table 4 shows the period and the corresponding modal participating mass ratio of each mode output from SAP. It shows that the first and second mode together include the 93% total modal participating mass. Therefore, it was considered that these two modes would govern the structure's performance under seismic events.

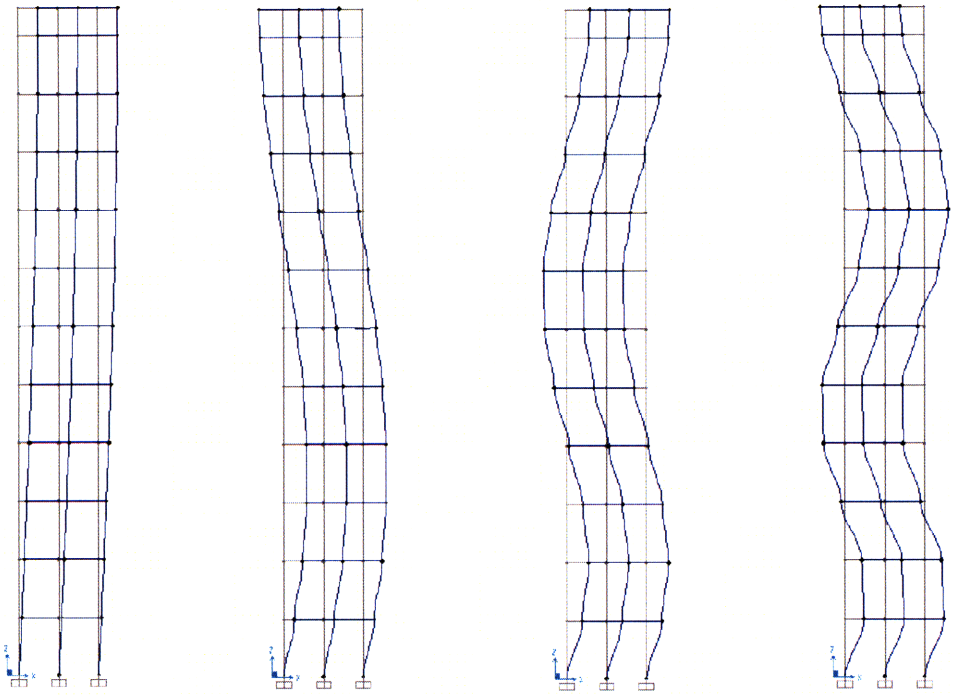

Figure 12: Mode shapes

Modal Participating Mass Ratios				
OutputCase	**StepType**	**StepNum**	**Period**	**UX**
Text	Text	Unitless	Sec	Unitless
MODAL	Mode	1	6.767254	0.811055
MODAL	Mode	2	2.364363	0.121092
MODAL	Mode	3	1.449576	0.036753
MODAL	Mode	4	1.04231	0.014915
MODAL	Mode	5	0.832168	0.008666
MODAL	Mode	6	0.705553	0.004553
MODAL	Mode	7	0.623634	0.002409
MODAL	Mode	8	0.569997	0.000516
MODAL	Mode	9	0.519712	0.000037
MODAL	Mode	10	0.482246	0.00000342

Table 4: Period and modal participating mass ratios of the first 10 modes

5.3 Wind

5.3.1 Periodic function

To represent the wind excitation the building is under, a sinusoidal function with a frequency identical to the fundamental frequency of the building was created (Figure 13). This function has the form of $p = \hat{p} \sin \Omega t$. The amplitude $\hat{p}$ was back-calculated based on the fact that the peak acceleration of the top occupied floor is 7.9 milli-g under the strongest wind storm expected to occur in half of a year [21]. This amplitude was applied to the wind periodic function during the time history analysis as a scale factor. However, it was realized that this periodic function (and the Time Hisotry Analysis which would be followed) might not be the best way to model the effect of wind on the building, because the peak could be easily missed. Therefore, a steady state function was used instead.

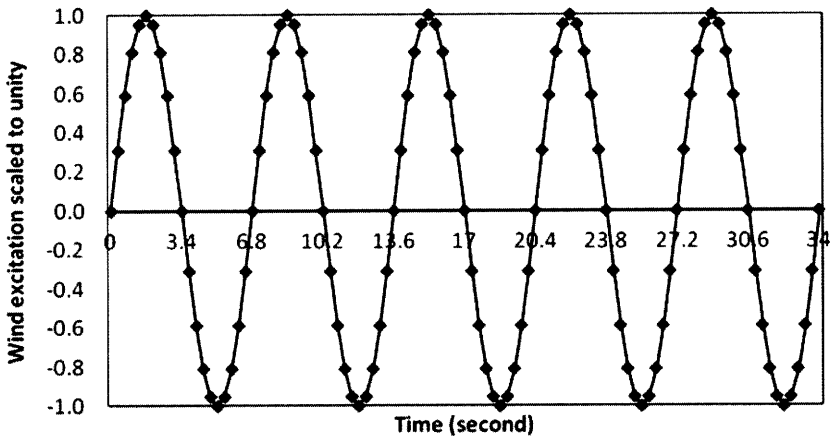

Figure 13: Periodic function used as wind excitation

5.3.2 Steady state function

The steady state function was used to capture the response of the building under all frequencies between 0.1 and 1Hz, which covers the first two modes of the building. The steady state function was a step function from value equal to 1 at frequency 0 to value equal to 1 at frequency 1.

5.3.3 Steady state analysis

The next step was to assign a load case for wind. It is a steady state analysis using direct integration as the solution type. The frequency ranges from 0.1Hz to 1Hz, with 100 time steps. This covers the all periods from 1 second to 10 seconds, which according to Table 4 is the first, second, third and the fourth mode. Appendix 3 shows the properties and values entered in SAP2000 Load Case Data. This can be verified by the four peaks in the acceleration plot of the top of the building shown in Figure 14. Finally, a scale factor was entered to achieve the 7 milli-g (0.069 m/sec2) peak acceleration at the top node of the model. Figure 15 shows the displacement plots of the top of the building.

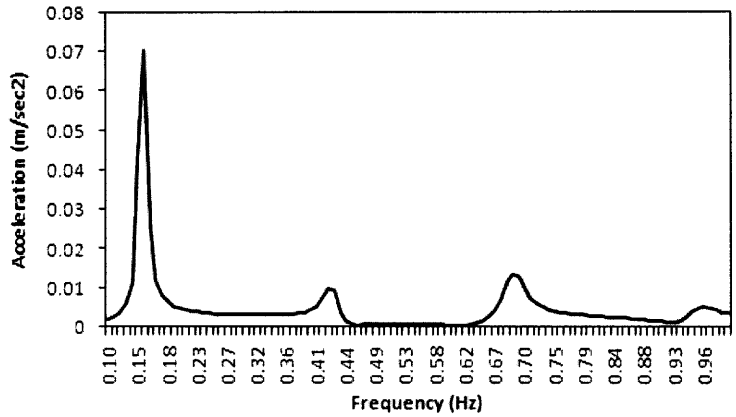

Figure 14: Acceleration at the top under wind excitation

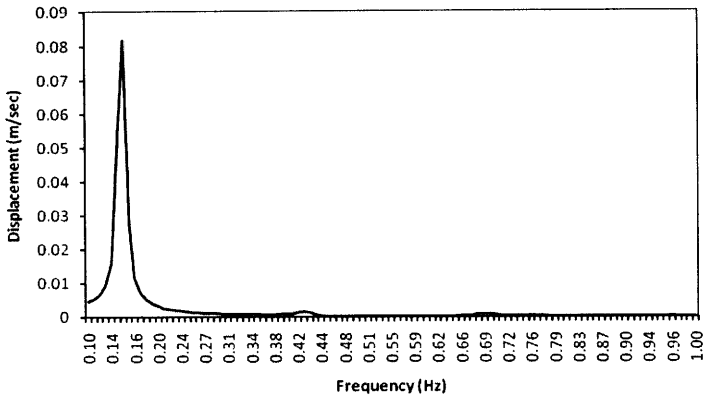

Figure 15: Displacement at the top under wind excitation

5.4 Earthquake

5.4.1 1999 Chi-chi earthquake data

A Mw7.6 earthquake occurred in Chi-Chi, Taiwan September 21 1999. For its main shock, 441 digital strong-motion records were processed from 663 data files by Taiwan Strong Motion Instrumentation Program (TSMIP) and Central Weather Bureau (CWB). The peak magnitude in Taipei ranged between 4 and 5.

Out of the 663 data files, the ones for Taipei region were extracted. Finally the two closest to Taipei 101 were compared, and the one with higher peak amplitude was selected for the analysis. Amplitude was measured in vertical (41.52 gal, or 39 milli-g), north-south (114.9 gal, or 108 milli-g), and east-west (88.7 gal, or 83 milli-g) directions. The record length was 120 seconds, and the time step was 0.005 seconds. For this location, the peak amplitude in north-south direction was higher than it in east-west direction. Therefore, the amplitude in north-south direction was used in the analysis. Figure 16 shows the ground accelerations in all three directions. Figure 17 shows the SAP Time History Function Definition of the seismic data.

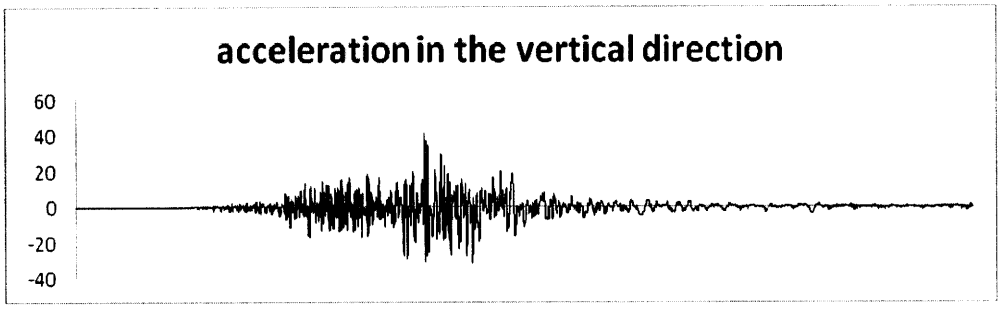

(a)

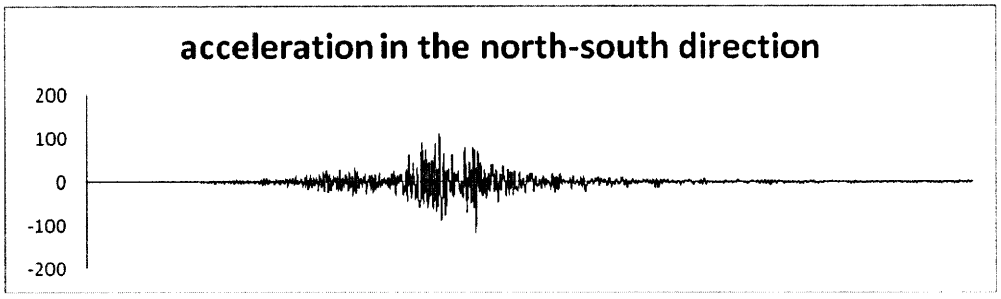

(b)

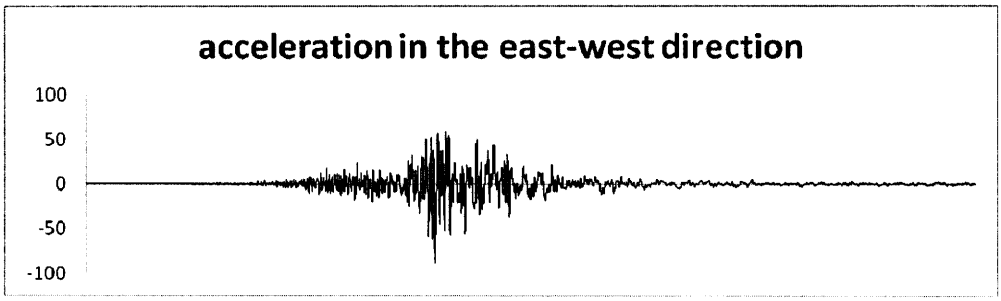

(c)

Figure 16: Chi-chi earthquake time history in all 3 directions

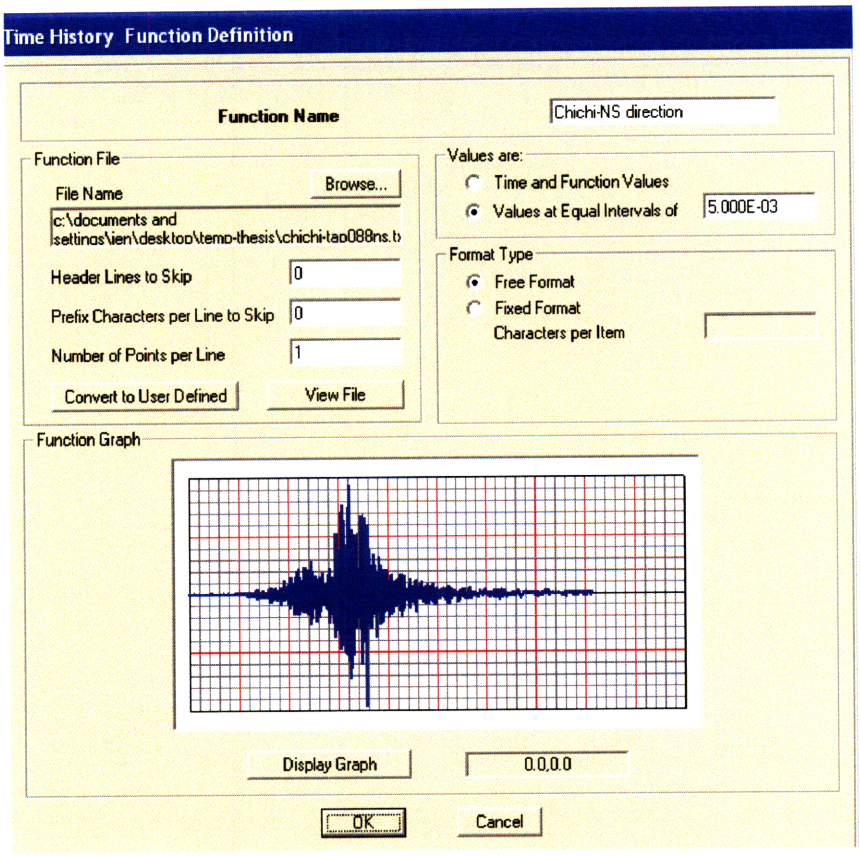

Figure 17: SAP Time history function definition

5.4.2 Time history analysis

The next step was to assign a load case for seismic. It is a linear, modal, transient time history analysis. The time step was taken to be 0.01, twice of the time step of the raw seismic data. The number of output time steps was the total analysis time 60 seconds divided by 0.01, which was equal to 6000 steps. Only the first 60 seconds was taken because the peak amplitude occurred in the first 60 seconds. Appendix 3 shows the properties and values entered in SAP 2000 Load Case Data. The acceleration and displacement at the top node of the model was shown in Figure 18 and Figure 19. The peak acceleration is 105 gal. The peak displacement is 12.89 meters. The maximum base shear is 2,543,893 tons. The maximum moment at the base is 391,835,584 ton-

meter. The peak acceleration, the maximum base shear, and the maximum moment at the base will be compared later with the case when the TMD is in use.

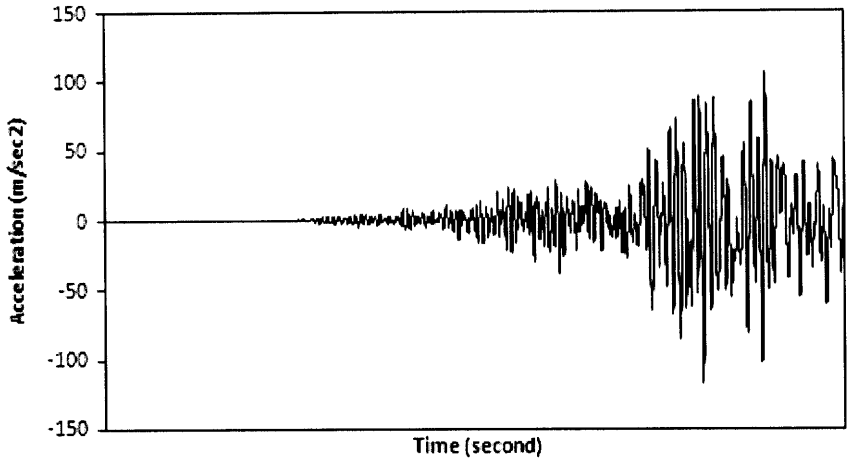

Figure 18: Acceleration at the top under seismic excitation

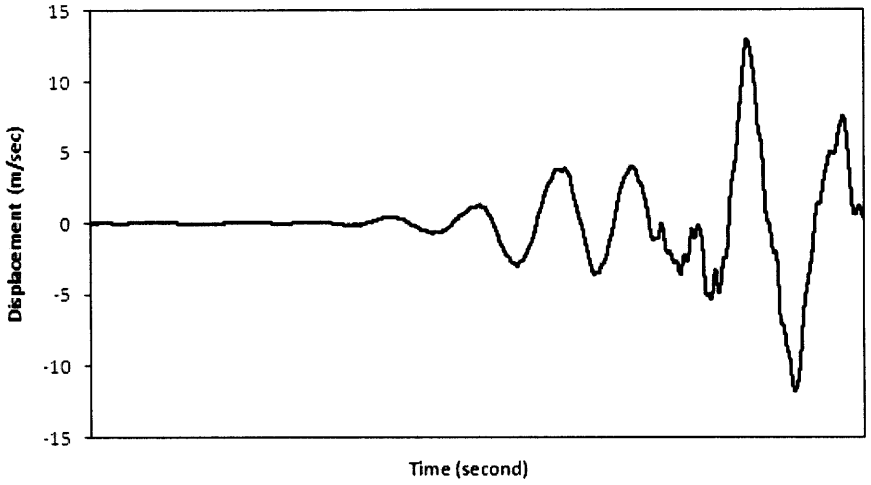

Figure 19: Displacement at the top under seismic excitation

6. Taipei 101: Analysis

6.1 Tuned mass damper system

The actual TMD has a length of 11.5 meters and a mass of 700 tons. It was modeled as an NLLink element in SAP2000 attached to a top-storey column. The NLLink element has an effective damping and effective stiffness defined as follows: the effective stiffness K_{eq} is W_d/L for pendulum-type TMDs, where W_d is the weight of the TMD. The effective damping C is $2\xi(km)^{1/2}$ [Connor]. Then a point mass was added to the free end of the NNlink element to represent the pendulum-type TMD. The mass of the TMD is 700 tons, 0.26% of the structural mass. With the added damper mass, the fundamental period of the building is increased from 6.7 seconds to 7.0 seconds. See Figure 20 for the detail of the TMD model.

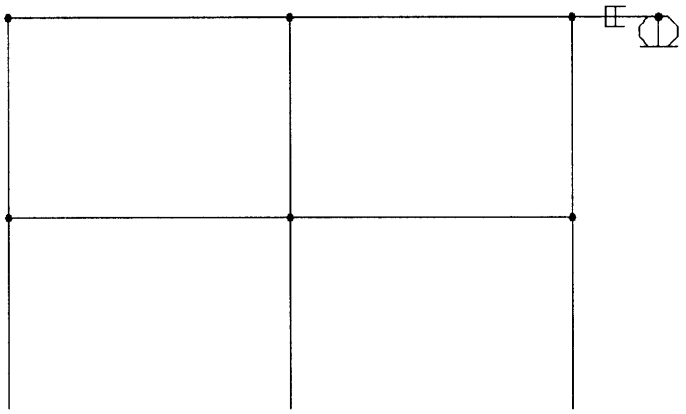

Figure 20: SAP 200 Model with TMD

6.1.1 Structural response under wind

The peak acceleration of the top node of the model was reduced by 33% from 7 milli-g (0.069 m/sec2) to 4.7 milli-g (0.046 m/sec2), which is close to the peak acceleration (5.0 milli-g) of the

actual building (Figure 21). The peak displacement of the top mode was reduced by 32% from 0.082m to 0.056m (Figure 22).

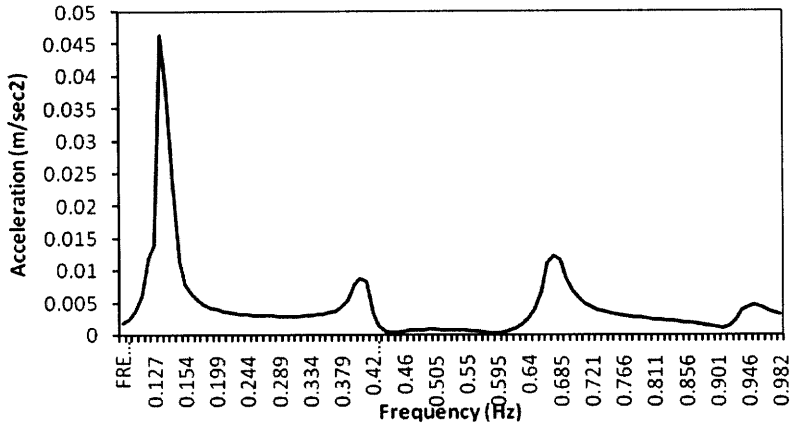

Figure 21: Acceleration at the top under wind excitation

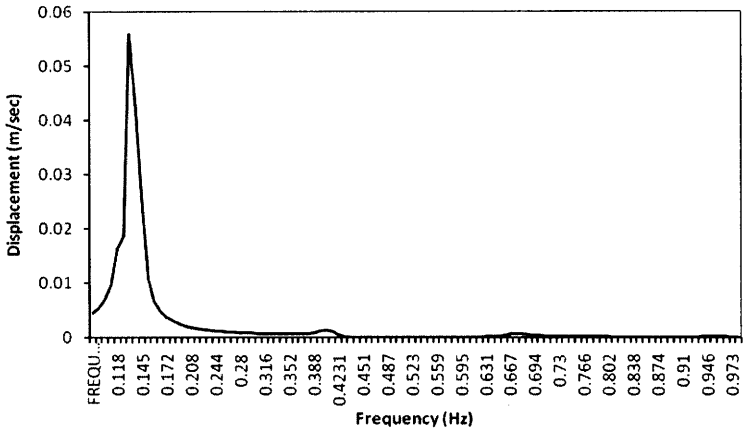

Figure 22: Displacement at the top under wind excitation

6.1.2 Structural response under seismic

With a 1.5% modal damping, the acceleration and displacement at the top node of the model was shown in Figure 23 and 24. The peak acceleration was increased by 4.76% from 105 gal to 110 gal. The peak displacement was reduced by 0.85% from 12.89 meters to 12.78 meters. The maximum base reaction was reduced by 2.18% from 2,543,893 tons to 2,488,538tons. The

maximum moment at the base was increased by 4.76% from 391,835,584 ton-meter to 410,506,289 ton-meter.

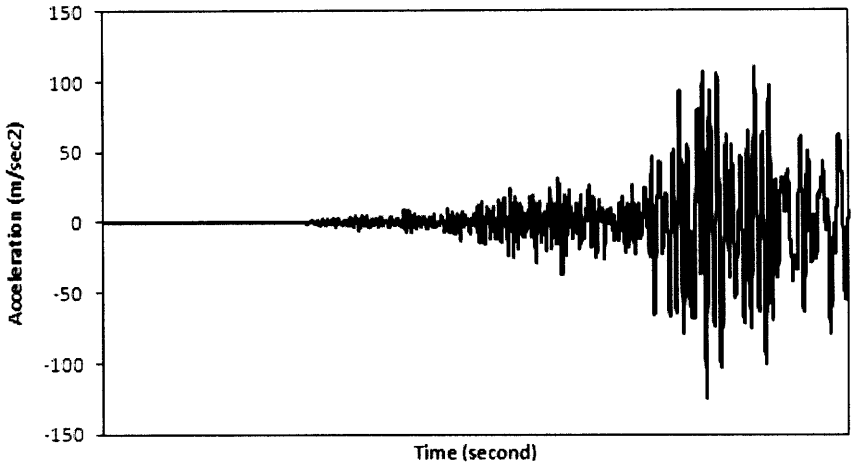

Figure 23: Acceleration at the top under seismic excitation

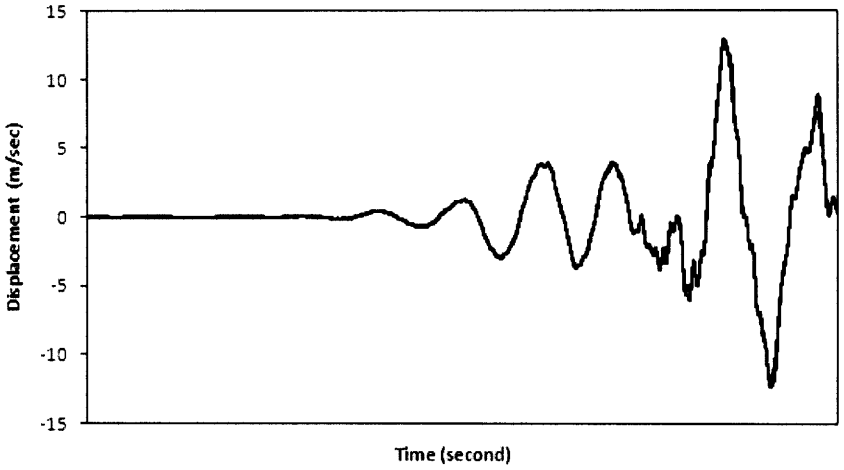

Figure 24: Displacement at the top under seismic excitation

6.1.3 Sensitivity study

To assess the effect of the TMD mass on the structural response, a sensitivity study was performed to compare the structural response with different mass ratios: No TMD (0%), 385-ton

TMD (0.13%), 770-ton TMD (0.26%), 2960-ton TMD (1.00%), and 7700-ton TMD (2.60%). The structural response at each storey was plotted for each mass ratio, as shown in Figure 25 and 26. The maximum displacement and accelerations were reduced as the TMD mass increases under wind excitation. However, TMD is relatively ineffective when the building is under seismic excitation, and in some cases produce a negative effect, as shown in Figure 27 and 28.

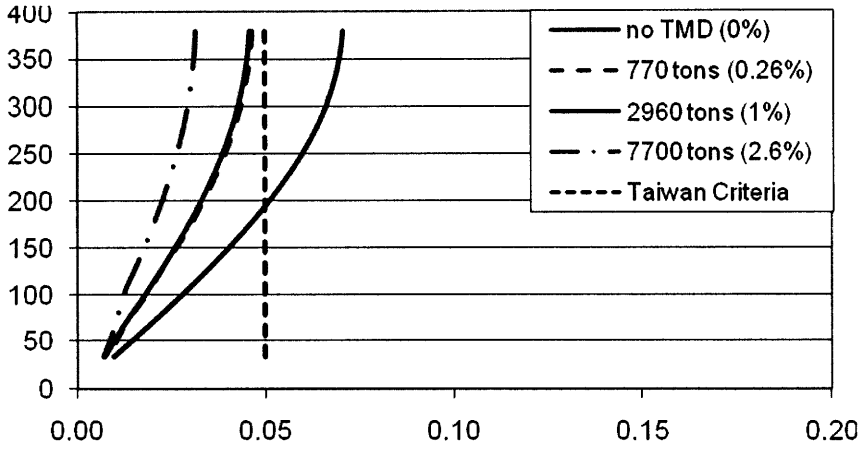

Figure 25: Acceleration (m/sec2) along building height (m) under wind excitation

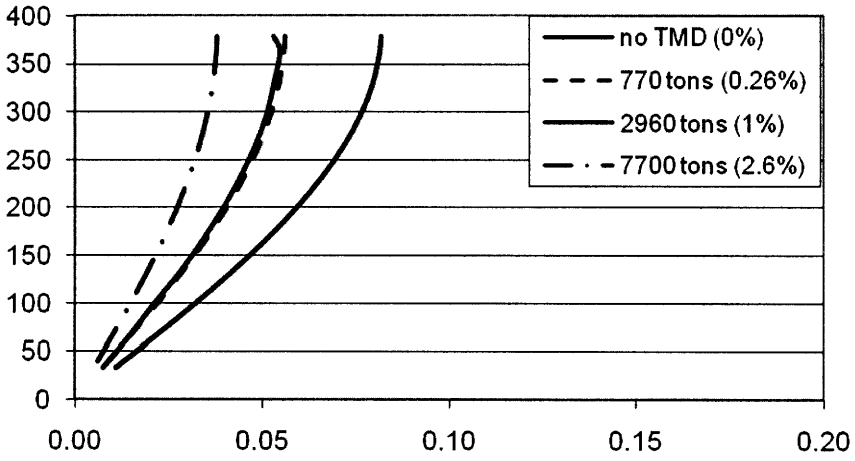

Figure 26: Displacement (m/sec) along building height (m) under wind excitation

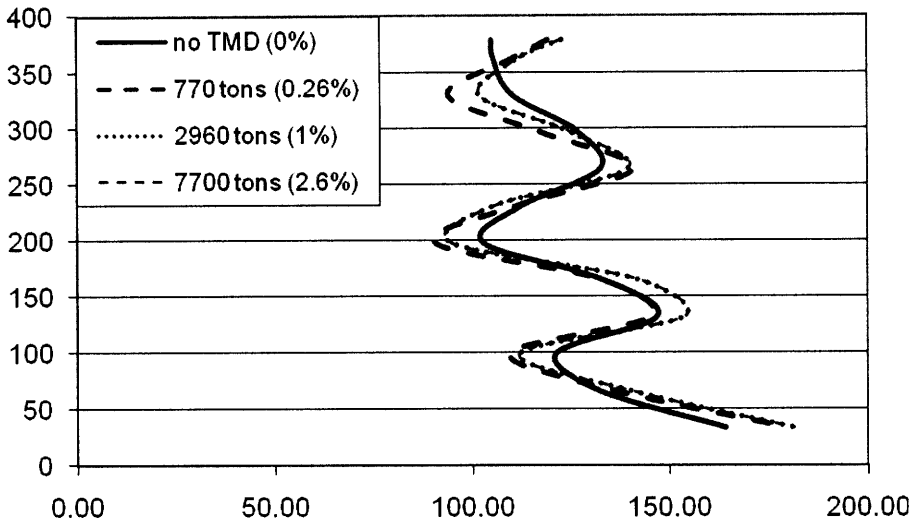

Figure 27: Acceleration (m/sec2) along building height (m) under seismic excitation

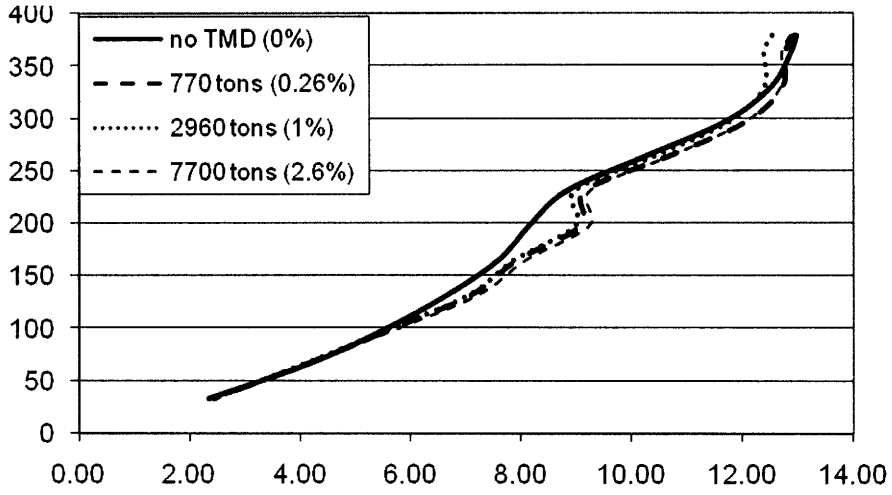

Figure 28: Displacement (m/sec) along building height (m) under seismic excitation

6.1.4 Effectiveness of a second TMD

There have been several studies on the effectiveness of placing several TMDs in a building. Here, a second TMD was placed to study its effectiveness of the structural response. It has been established that TMD is not as effective in reducing the structural response under seismic, so

only the response under wind was of interest. A second TMD was placed at where the maximum displacement occurs in the second mode (approximately 120m) with a mass of 100 tons, compared to the first TMD (approximately 379m) with a mass of 770 tons, as shown in Figure 29.

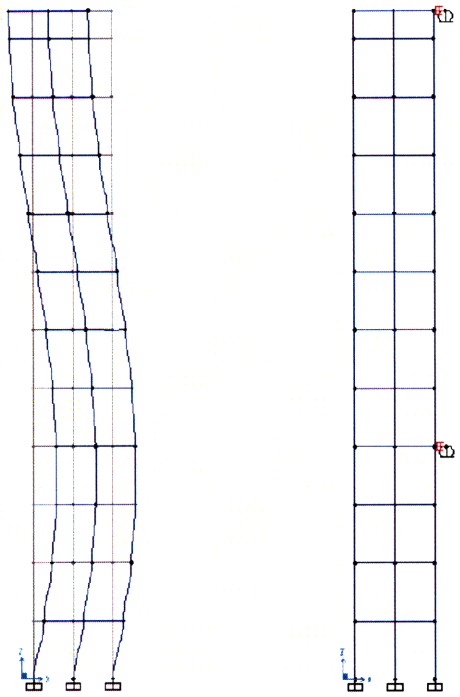

Figure 29: Location of the second TMD

Figure 30 and 31 shows the maximum displacement and acceleration along the height of the building without TMD, with the existing 770-ton TMD, and with two TMDs. The reductions are hardly noticeable. The reason is likely that the mass participation ratio of the second mode is significantly lower than that of the first mode (12% compared to 81%), therefore the second mode affects the motion of the building much less than the first mode. Placing a TMD for the second mode would not reduce the structural response much.

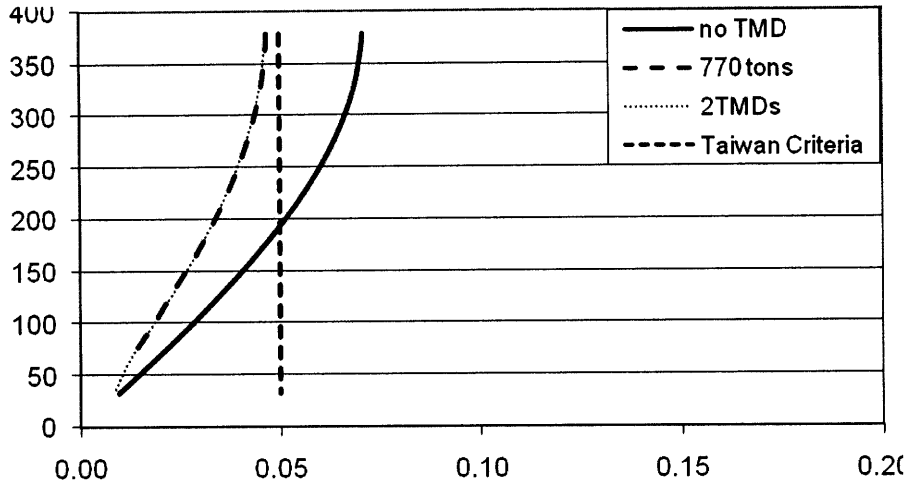

Figure 30: Acceleration (m/sec2) along building height (m) under wind excitation

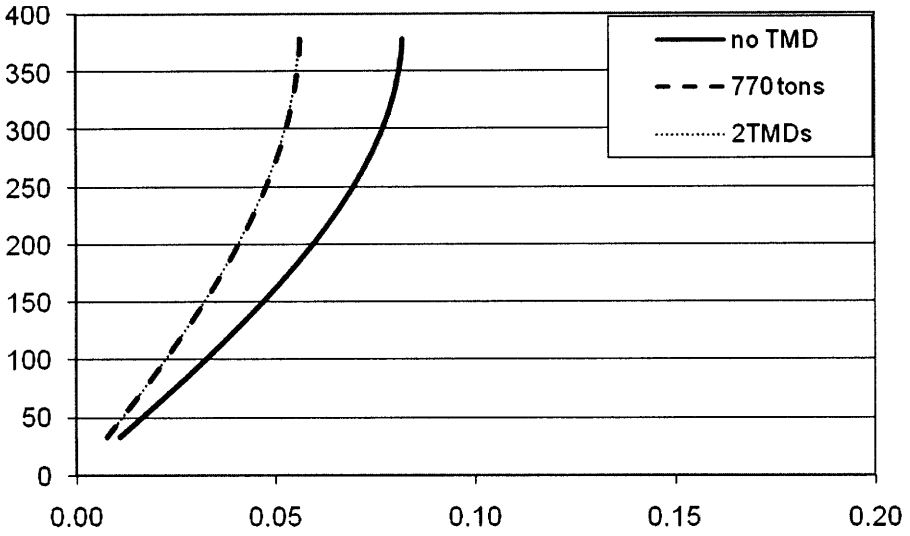

Figure 31: Displacement (m/sec) along building height (m) under wind excitation

6.2 Viscous damper system

After the demonstration of the effectiveness of TMD systems, viscous damper systems were also studied. The performance of viscous dampers depends on the relative velocity. A common location for viscous dampers is where cross bracings are in the outriggers. However, the

constructability of such a damper is complicated, and not every building has cross bracings. An innovative system has been invented by Arup, in which viscous dampers are placed in the outrigger-column connection, as shown in Figure 32. Figure 33 shows the relation between the damping force and the relative velocity of a damper under wind and seismic action.

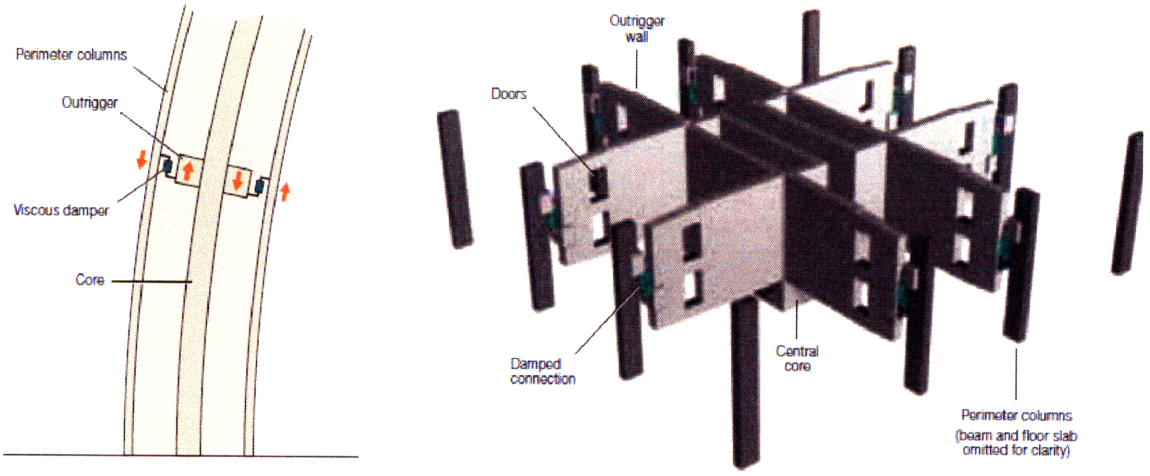

Figure 32: Outrigger viscous dampers scheme by Arup [22]

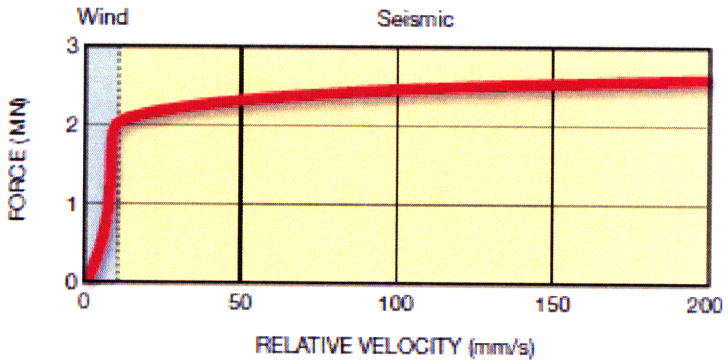

Figure 33: The relation between damping force and the relative velocity of a damper [22]

The outriggers connect the core to the perimeter columns, transferring the lateral load through shear forces. Therefore, that is an excellent location for placing dampers. As shown in Figure 34,

dampers were inserted as NLLink elements in the middle of the outriggers in SAP2000. The actual physical location of the outriggers would be between the column and the end of the outrigger, but they were placed in the middle for modeling purposes. This assumption would have some minor impacts on the analysis results.

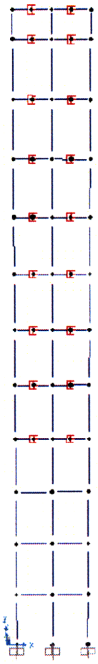

Figure 34: SAP2000 model with viscous dampers

A parametric study was performed to demonstrate the effectiveness of the outriggers. The benchmark was the base shear due to seismic excitation from the time history analysis. It was found that the base shear decreased as the value for C increased. However, there is an upper and lower bound of the efficiency of the damper. A reduction of approximately 22% in the maximum base shear over the time history was observed.

6.2.1 Structural response under wind

Accelerations due to wind excitation were compared for the building without dampers, with TMD and with viscous dampers schemes. The results are shown in Figure 35. The structural response is reduced with TMD, and reduced even more with viscous dampers. Of course, the relative difference between TMD and viscous dampers scheme depends on the size of the dampers used.

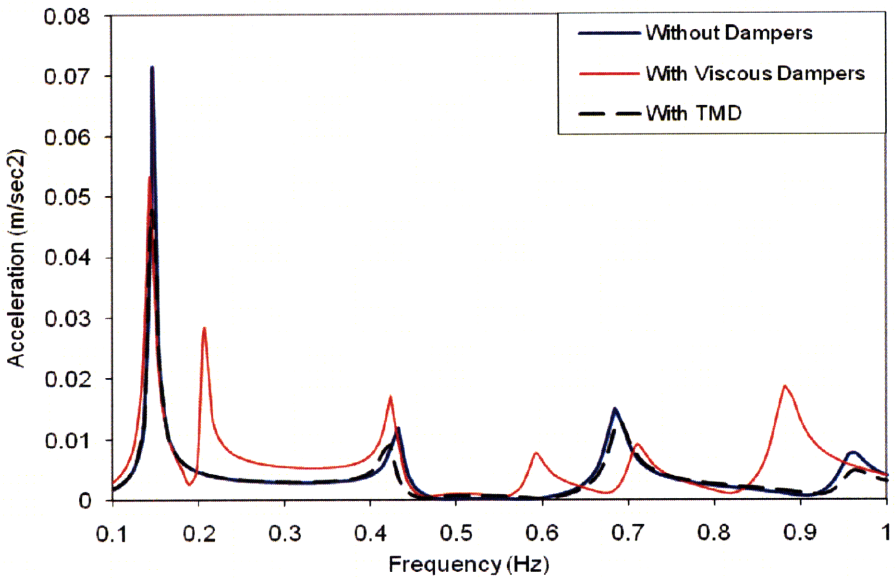

Figure 35: Accelerations with and without dampers under wind excitation

6.2.2 Structural response under seismic

Base shears due to seismic excitation were compared for the building without dampers, with TMD and with viscous dampers schemes. The results are shown in Figure 36. The structural response is reduced with TMD, and reduced even more with viscous dampers. This is a reasonable result because viscous dampers usually work much more effectively than TMDs.

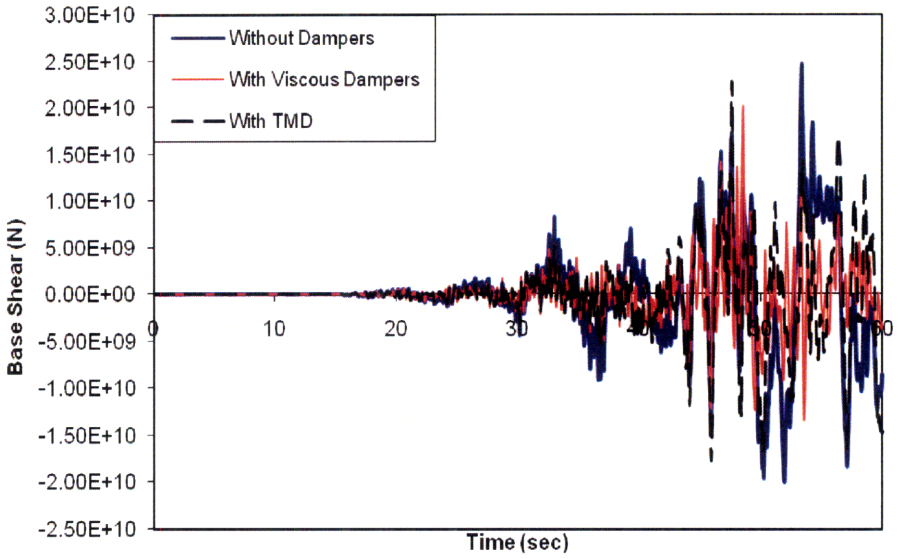

Figure 36: Base shear with and without dampers under seismic excitation

7. Conclusions

The design concept and procedure, as well as current applications of tuned mass and viscous dampers have been compared. A design summary of Taipei101 in terms of its structural system, specifically its wind and seismic design were explained. Taipei101 was then modeled in a two-dimensional scheme in SAP2000 and calibrated based on the known structural responses under wind and seismic excitations.

After the design summary and model calibration, a TMD was then placed on the top of Taipei101 to study its effect on the structural response due to wind and seismic excitations and confirm with the actual effect. A sensitivity study was then performed to study the effect of mass ratio on the structural response. Results showed that increasing mass ratio would increase the effectiveness of TMDs under wind excitations, but not as effective under seismic excitations. This is as expected because TMDs are mostly designed to reduce motion under wind excitations. A second TMD was then placed at the location where the maximum deflection occurs for the second mode. Results showed that adding a second TMD would not reduce the structural response by much. This was possibly due to the fact that the first mode of this model had a mass participating ratio of over 80%. Therefore, the first mode governed. Finally, 12 viscous dampers were placed in Taipei101 to study their effects on the structural response due to wind and seismic excitations. Time-history and steady-state analysis in SAP2000 were used for all the wind and seismic analyses.

8. References

[1] Kareem, A. 1982 Fluctuating wind load on buildings. *Journal of Engineering Mechanics, ASCE* **EM6**: 1086–1102.

[2] Kawai, H. 1993 Bending and torsional vibration of tall building in strong wind. *Journal of Wind Engineering and Industrial Aerodynamics* **50**: 281–288.

[3] Simiu, E. 1996. Wind Effect on Structures (3rd edn). Wiley: New York.

[4] Kwok, K.C.S. & Samali, B., 1995 Performance of tuned mass dampers under wind loads, *Engineering Structures,* Vol. 17, No. 9, 655~67

[5] McNamara, RJ. 1977 Tuned mass damper for buildings. *Journal of Structural Engineering, ASCE* **103(9):** 1785–1798.

[6] Kim, Y.M., You, K.P., & Kim, H.Y., 2008 Wind-induced excitation control of a tall building with tune mass dampers. *Struct. Design Tall Spec. Build.* **17**, 669–682

[7] Lee, C.L. et al. 2006 Optimal design theories and applications of tuned mass dampers, *Engineering Structures* **28** 43–53

[8] Connor, J. 2003 Introduction to Structural Motion Control, Prentice Hall: New Jersey

[9] Gamaliel, R. 2008 Frequency-based response of damped outrigger systems for tall buildings, M.Eng thesis, Massachusetts Institute of Technology, 12

[10] Xu, Y.L., Samali , B., & Kwok, K.C.S. 1992 Control of along-wind response of structures by mass and liquid dampers. *J. Engng Mech. ASCE* **118** 1, 20–39

[11]] Xu, Y.L., Kwok, K.C.S.& Samali , B., Control of wind-induced tall building vibration by tuned mass dampers. *J. Wind Engng Ind. Aerodyn.* **40** (1992), 1–32

[12] Kourakis, I. 2007 Structural systems and tuned mass dampers of super tall buildings: Case study of Taipei101, M.Eng thesis, Massachusetts Institute of Technology, 38-39

[13] Lavan, O. & Levy, R. 2006 Optimal design of supplemental viscous dampers for linear framed *structures Earthquake Engng Struct. Dyn.* **35**, 337–356

[14] Miyamoto, H.K. & Scholl, R.E. 1996 Case study: Seismic rehabilitation of non-ductile soft storey concrete structure using viscous dampers. Proceedings of the eleventh world conference on earthquake engineering, Paper No 315, Acapulco, Mexico. Elsevier Science: Amsterdam, June 23-28

[15] Taylor Device Inc. web, viewed May 10 May 2009 <http://www.taylordevices.com/>

[16] Constantinou, M.C. & Tadjbakhsh, I.G.1983 Optimum design of a first storey damping system. *Computers and Structures*, **17(2)**: 305 –310.

[17] Fu, Y. & Kasai,K. 1998 Comparative study of frames using viscoelastic and viscous dampers. *Journal of Structural Engineering* **124(5):** 513 –522.

[18] Joseph, L., Poon, D. & Shieh, S. 2006 Ingredients of High-rise Design. *Structure Magazine*, June, 40-45

[19] Shieh, S.S., Chang, C.C. & Jong, J.H. Structural design of Composite Super-columns for the Taipei101 tower, Courtesy of Evergreen Consulting Engineering, Inc. Taiwan

[20] Irwin, P.Developing Wind Engineering Techniques to Optimize Design and Reduce Risk. Courtesy of RWDI

[21] Haskett, T. et al. Tuned mass dampers under excessive structural excitation. Courtesy of Motioneering Inc.

[22] Smith, R. & Willford, M. 2008 Damped outriggers for tall buildings. *The Arup Journal*, 3: 17-19

Appendix 1: Chi-chi earthquake raw data

#StationCode: TAP088

#InstrumentKind: ETNA

(F7426301.EVT)

#StartTime: 1999/09/20-17:47:29.000

#RecordLength(sec): 122.00

#SampleRate(Hz): 200

#AmplitudeUnit: gal. DCoffset(corr)

#AmplitudeMAX. U: 41.512~ -31.201

#AmplitudeMAX. N: 112.322~ -115.015

#AmplitudeMAX. E: 59.292~ -88.792

#DataSequence: Time U(+); N(+); E(+)

#Data: 4F10.3

		highest peak accel. [gal]		[milli-g]
Time	U	NS	EW	NS
0	0	-0.005	0.001	-0.005
0.005	-0.005	-0.009	-0.008	-0.008
0.01	0	-0.002	-0.02	-0.002
0.015	-0.005	0.021	0.017	0.020
0.02	-0.003	0.014	0.011	0.013
0.025	-0.005	-0.003	-0.032	-0.003
0.03	-0.003	-0.004	0.007	-0.004
0.035	0.005	0.008	0.022	0.008
0.04	0.005	-0.001	0.009	-0.001
0.045	0.002	-0.005	0.007	-0.005
0.05	0.002	0.003	-0.01	0.003
0.055	0.009	0.001	0.007	0.001
0.06	0.006	0.016	0.033	0.015
0.065	0.003	-0.007	0.009	-0.007
0.07	-0.007	-0.005	-0.011	-0.005
0.075	0.005	0.006	0.005	0.006
0.08	0.008	-0.008	0.01	-0.008
0.085	-0.013	0.012	0.008	0.011
0.09	-0.005	0	-0.006	0.000
0.095	0.004	-0.013	-0.017	-0.012
0.1	0.002	-0.005	-0.002	-0.005

0.105	-0.001	0.009	0.008	0.008
0.11	-0.002	0.009	0.001	0.008
0.115	-0.011	-0.019	0.001	-0.018
0.12	-0.008	-0.023	0.011	-0.022
0.125	-0.001	0	0.01	0.000
0.13	-0.015	0.015	0.006	0.014
0.135	-0.008	-0.006	-0.005	-0.006
0.14	0.006	-0.006	-0.008	-0.006
0.145	0.002	0	-0.004	0.000
0.15	0.003	-0.017	0.006	-0.016
0.155	0.02	-0.005	0.018	-0.005
0.16	0.01	0.001	-0.005	0.001
0.165	0.005	-0.009	-0.014	-0.008
0.17	0.015	0.003	0.01	0.003
0.175	-0.006	-0.009	0.006	-0.008
0.18	-0.004	-0.017	-0.01	-0.016
0.185	0.002	-0.004	-0.003	-0.004
0.19	0.009	-0.007	0.006	-0.007
0.195	0.01	0.008	0.001	0.008
0.2	-0.002	0.014	-0.005	0.013
0.205	0.011	0.005	-0.002	0.005
0.21	-0.005	-0.007	0.003	-0.007
0.215	-0.007	-0.012	-0.001	-0.011
0.22	0.002	-0.017	-0.007	-0.016
0.225	-0.009	-0.017	-0.011	-0.016
0.23	0.002	0.012	-0.002	0.011
0.235	-0.005	0	-0.011	0.000
0.24	-0.009	-0.007	-0.011	-0.007
0.245	0.001	0.001	0.013	0.001
0.25	-0.007	-0.011	-0.007	-0.010
0.255	-0.005	-0.011	-0.025	-0.010
0.26	-0.001	-0.011	-0.012	-0.010
0.265	0	0.005	0.003	0.005
0.27	0.007	0.008	0.006	0.008
0.275	0.002	0.007	-0.016	0.007
0.28	-0.006	0.005	-0.003	0.005
0.285	0	0.005	0.017	0.005
0.29	-0.007	0.022	-0.001	0.021
0.295	0.006	0.001	-0.006	0.001
0.3	0.008	0.008	0.004	0.008

Appendix 2: Taipei101 Modal Calibration

TMD			
mass	730,000	kg	kg
T	6.8	sec	sec
L	11.5	m	m
Keq	623	kN/m	
ksi	0.047		
C	2004		

Earthquake		
no. of steps	7000	
step size	0.01	(=2*0.005) twice of earthquake data
duration	70	sec
scale factor	1	

Wind		
no. of steps	170	
step size	0.2	
duration	34	sec
scale factor	25000	

Acceleration				
top floor (no TMD)	7.9	milli-g	0.077	m/sec^2
top floor (TMD)	5	milli-g	0.049	m/sec^2
Taiwan criteria	5.1	milli-g	0.050	m/sec^2

Super-columns (SC)

Young's Modulus			Density				
Steel	200	Gpa	LWC slab	1900	[kg/m^3]		steel
HSC	30	GPa	HSC	2400	[kg/m^3]		steel+HSC
ratio	6.67		Steel	7800	[kg/m^3]	Steel thickness	0.08 [

Cross-section		Area (actual)		Area (trans)	a	Ixx total = bh^3/12+A*a^2		
b [m]	h [m]	Steel [m^2]	HSC [m^2]	[m^2]	[m]	[m^4]		
2	1.6	0.58	0	3.84	23	2032	2	4064
					11	465	2	931
						total/SAP column		4995
2	1.6	0.58	0	3.84	23	2032	2	4064
					11	465	2	931
						total/SAP column		4995
2.2	1.8	0.64	0	4.27	23	2258	2	4516
					11	517	2	1035
						total/SAP column		5551
2.4	2	0.70	0	4.69	23	2484	2	4969
					11	569	2	1139
						total/SAP column		6108
2.4	2	0.70	4.8	9.49	23	5024	2	10047
					11	1150	2	2301
						total/SAP column		12348
2.6	2.2	0.77	5.72	10.84	23	5737	2	11473
					11	1314	2	2628
						total/SAP column		14101
3	2.4	0.86	7.2	12.96	23	6859	2	13719
					11	1572	2	3143
						total/SAP column		16862
3	2.4	0.86	7.2	12.96	23	6859	2	13719
					11	1572	2	3143
						total/SAP column		16862
3	2.4	0.86	7.2	12.96	23	6859	2	13719
					11	1572	2	3143
						total/SAP column		16862
3	2.4	0.86	7.2	12.96	23	6859	2	13719
					11	1572	2	3143
						total/SAP column		16862

m(slab1) [kg]	d(slab1) [m]	m(slab2) [kg]	d(slab2) [m]	Jzz(slab) [kg-m^4]	zz(slab eff [kg-m^4]	m(1sc) [kg]	Jzz(sc) [kg-m^4]	Jzz(sc eff) [kg-m^4]	Jzz (total) [kg-m^4]
72105	20	72105	5.5	71,582,239	5,368,668	147,456			
							220,326,789	220,326,789	225,695,457
72105	20	72105	5.5	71,582,239	2,602,991	304,128			
							454,424,003	454,424,003	457,026,993
72105	20	72105	5.5	71,582,239	2,602,991	337,920			
							505,086,771	505,086,771	507,689,762
72105	20	72105	5.5	71,582,239	2,602,991	371,712			
							555,803,607	555,803,607	558,406,598
72105	20	72105	5.5	71,582,239	2,602,991	751,872			
							1,124,239,114	1,124,239,114	1,126,842,105
72105	20	72105	5.5	71,582,239	2,602,991	858,528			
							1,284,243,418	1,284,243,418	1,286,846,408
72105	20	72105	5.5	71,582,239	2,602,991	1,026,432			
							1,536,486,589	1,536,486,589	1,539,089,580
72105	20	72105	5.5	71,582,239	2,602,991	1,026,432			
							1,536,486,589	1,536,486,589	1,539,089,580
72105	20	72105	5.5	71,582,239	2,602,991	1,026,432			
							1,536,486,589	1,536,486,589	1,539,089,580
72105	20	72105	5.5	71,582,239	2,791,707	3,110,400			
							4,656,019,968	4,656,019,968	4,658,811,675

Floor	Height [m]	column dim [m]	Area	Ixx [m^4]	Jzz [ton-m^4]
90-101	16	2.0x1.6	3.84	4,995	225,695
82-90	33	2.0x1.6	3.84	4,995	457,027
74-82	33	2.2x1.8	4.27	5,551	507,690
66-74	33	2.4x2.0	4.69	6,108	558,407
58-66	33	2.4x2.0	9.49	12,348	1,126,842
50-58	33	2.6x2.2	10.84	14,101	1,286,846
42-50	33	3.0x2.4	12.96	16,862	1,539,090
34-42	33	3.0x2.4	12.96	16,862	1,539,090
26-34	33	3.0x2.4	12.96	16,862	1,539,090
0-26	100	3.0x2.4	12.96	16,862	4,658,812

Core-columns (SC)

Young's Modulus			Density		
Steel	200	Gpa	LWC slab	1900	[kg/m^3]
HSC	30	GPa	HSC	2400	[kg/m^3]
ratio	6.67		Steel	7800	[kg/m^3]

(blank)	steel		
(shaded)	steel+HSC		
Steel thickness		0.08	[m]

Cross-section		Area (actual)		Area (trans)	a	Ixx total = bh^3/12+A*a^2			m(1CC)	Jzz(CC)
b [m]	h [m]	Steel [m^2]	HSC [m^2]	[m^2]	[m]	[m^4]			[kg]	[kg-m^4]
1.00	1.00	0.32	0	2.13	11	258	8	2066	81,920	
					5	53	8	427		
						total/SAP column		2493		417,355,093
1.00	1.00	0.32	0	2.13	11	258	8	2066	168,960	
					5	53	8	427		
						total/SAP column		2493		860,794,880
1.10	1.10	0.35	0	2.35	11	285	8	2280	186,439	
					5	59	8	472		
						total/SAP column		2751		949,950,809
1.33	1.33	0.43	0	2.84	11	344	8	2752	225,012	
					5	71	2	143		
						total/SAP column		2895		1,146,825,947
1.33	1.33	0.43	1.77	4.61	11	559	8	4469	365,477	
					5	116	2	231		
						total/SAP column		4700		1,862,739,885
1.33	1.33	0.42	1.76	4.59	11	556	8	4450	363,898	
					5	115	8	921		
						total/SAP column		5371		1,854,677,843
1.48	1.48	0.47	2.20	5.36	11	649	8	5193	424,654	
					5	134	8	1076		
						total/SAP column		6269		2,164,827,286
1.48	1.48	0.47	2.20	5.36	11	649	8	5193	424,654	
					5	134	8	1076		
						total/SAP column		6269		2,164,827,286
1.48	1.48	0.47	2.20	5.36	11	649	8	5193	424,654	
					5	134	8	1076		
						total/SAP column		6269		2,164,827,286
1.48	1.48	0.47	2.20	5.36	11	649	8	5193	#######	
					5	134	8	1076		
						total/SAP column		6269		6,560,082,684

Floor	Height	:olumn Dime	Area	no. CC	Total Area	Ixx	Jzz
	[m]	[m]				[m^4]	[ton-m^4]
90-101	16	1.0x1.0	2.13	16	34.13	2,493	417,355
82-90	33	1.0x1.0	2.13	16	34.13	2,493	860,795
74-82	33	1.1x1.1	2.35	16	37.66	2,751	949,951
66-74	33	1.3x1.3	2.84	16	45.46	2,895	1,146,826
58-66	33	1.3x1.3	4.61	16	73.83	4,700	1,862,740
50-58	33	1.3x1.3	4.59	16	73.51	5,371	1,854,678
42-50	33	1.48x1.48	5.36	16	85.79	6,269	2,164,827
34-42	33	1.48x1.48	5.36	16	85.79	6,269	2,164,827
26-34	33	1.48x1.48	5.36	16	85.79	6,269	2,164,827
0-26	100	1.48x1.48	5.36	16	85.79	6,269	6,560,083

Appendix 3: Load case definition

Steady state load case

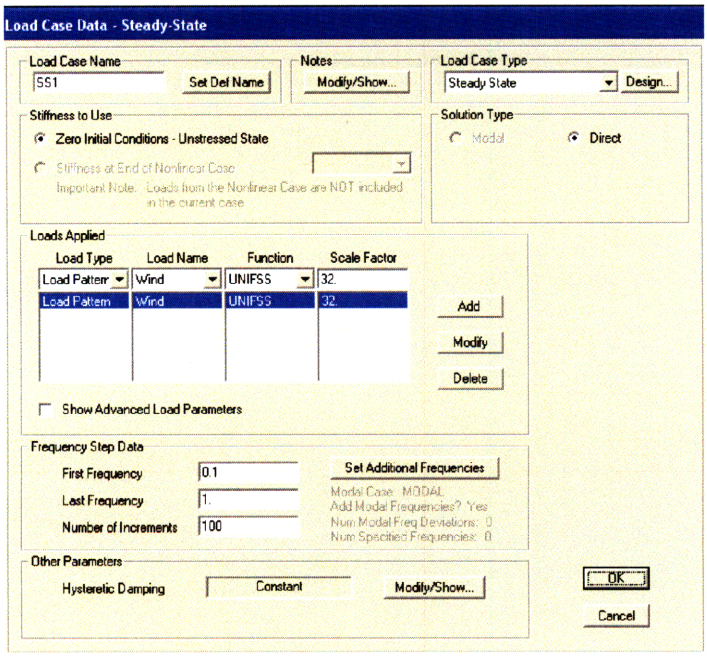

Time history load case

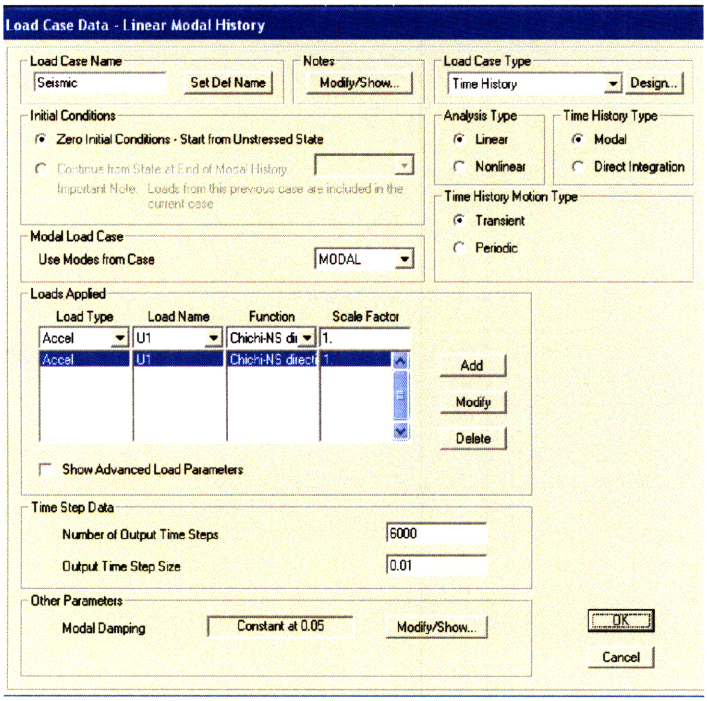

Appendix 4: Joint acceleration at the top with different dampings

TABLE: Joint Accelerations - Relative_No TMD						
Joint	OutputCase	CaseType	StepType	U1	U2	U3
Text	Text	Text	Text	m/sec2	m/sec2	m/sec2
3	Seismic	LinModHist	Max	104.93355	0	0.01962
32	Seismic	LinModHist	Max	105.39912	0	0.01916
33	Seismic	LinModHist	Max	110.27351	0	0.01728
34	Seismic	LinModHist	Max	127.01066	0	0.01484
35	Seismic	LinModHist	Max	132.66059	0	0.01214
36	Seismic	LinModHist	Max	112.49829	0	0.0106
37	Seismic	LinModHist	Max	102.75521	0	0.00909
38	Seismic	LinModHist	Max	133.1127	0	0.00774
39	Seismic	LinModHist	Max	146.89852	0	0.00629
40	Seismic	LinModHist	Max	121.10597	0	0.00477
41	Seismic	LinModHist	Max	132.24077	0	0.0032
44	Seismic	LinModHist	Max	164.07581	0	0.00161

TABLE: Joint Accelerations - Relative_770 tons						
Joint	OutputCase	CaseType	StepType	U1	U2	U3
Text	Text	Text	Text	m/sec2	m/sec2	m/sec2
3	Seismic	LinModHist	Max	119	0	0.0403
32	Seismic	LinModHist	Max	110	0	0.03934
33	Seismic	LinModHist	Max	94	0	0.03536
34	Seismic	LinModHist	Max	117	0	0.03024
35	Seismic	LinModHist	Max	141	0	0.02464
36	Seismic	LinModHist	Max	111	0	0.02146
37	Seismic	LinModHist	Max	91	0	0.01835
38	Seismic	LinModHist	Max	133	0	0.01559
39	Seismic	LinModHist	Max	146	0	0.01266
40	Seismic	LinModHist	Max	109	0	0.0096
41	Seismic	LinModHist	Max	136	0	0.00644
44	Seismic	LinModHist	Max	179	0	0.00323

TABLE: Joint Accelerations - Relative_2960 tons						
Joint	OutputCase	CaseType	StepType	U1	U2	U3
Text	Text	Text	Text	m/sec2	m/sec2	m/sec2
3	Seismic	LinModHist	Max	122.57017	0	0.04092
17	Seismic	LinModHist	Max	111.43317	0	0
32	Seismic	LinModHist	Max	111.60576	0	0.03994
33	Seismic	LinModHist	Max	101.59282	0	0.03592
34	Seismic	LinModHist	Max	124.63912	0	0.03073
35	Seismic	LinModHist	Max	139.46793	0	0.02505
36	Seismic	LinModHist	Max	105.32703	0	0.02183
37	Seismic	LinModHist	Max	94.45427	0	0.01867
38	Seismic	LinModHist	Max	142.07683	0	0.01586
39	Seismic	LinModHist	Max	153.76744	0	0.01289
40	Seismic	LinModHist	Max	111.8471	0	0.00978
41	Seismic	LinModHist	Max	140.08303	0	0.00656
44	Seismic	LinModHist	Max	181.32699	0	0.00329

TABLE: Joint Accelerations - Relative_7700 tons						
Joint	OutputCase	CaseType	StepType	U1	U2	U3
Text	Text	Text	Text	m/sec2	m/sec2	m/sec2
3	Seismic	LinModHist	Max	122.42491	0	0.04098
32	Seismic	LinModHist	Max	112.01795	0	0.04001
33	Seismic	LinModHist	Max	101.91584	0	0.03597
34	Seismic	LinModHist	Max	124.94215	0	0.03078
35	Seismic	LinModHist	Max	139.78385	0	0.02509
36	Seismic	LinModHist	Max	105.61964	0	0.02186
37	Seismic	LinModHist	Max	94.66863	0	0.01871
38	Seismic	LinModHist	Max	142.34815	0	0.01589
39	Seismic	LinModHist	Max	154.00605	0	0.01291
40	Seismic	LinModHist	Max	111.97951	0	0.00979
41	Seismic	LinModHist	Max	140.22558	0	0.00657
44	Seismic	LinModHist	Max	181.40664	0	0.0033

Appendix 5: Joint displacement at the top with different dampings

TABLE: Joint Displacements_no damping						
Joint	OutputCase	CaseType	StepType	U1	U2	U3
Text	Text	Text	Text	m	m	m
3	Seismic	LinModHist	Max	12.994941	0	0.002052
32	Seismic	LinModHist	Max	12.891349	0	0.002013
33	Seismic	LinModHist	Max	12.532506	0	0.001853
34	Seismic	LinModHist	Max	11.702207	0	0.001638
35	Seismic	LinModHist	Max	10.262005	0	0.001385
36	Seismic	LinModHist	Max	8.835551	0	0.00123
37	Seismic	LinModHist	Max	8.163568	0	0.001071
38	Seismic	LinModHist	Max	7.598439	0	0.000923
39	Seismic	LinModHist	Max	6.675982	0	0.000759
40	Seismic	LinModHist	Max	5.532076	0	0.000583
41	Seismic	LinModHist	Max	4.153042	0	0.000395
44	Seismic	LinModHist	Max	2.338086	0	0.000199

TABLE: Joint Displacements_770tons						
Joint	OutputCase	CaseType	StepType	U1	U2	U3
Text	Text	Text	Text	m	m	m
3	Seismic	LinModHist	Max	12.945841	0	0.002299
32	Seismic	LinModHist	Max	12.781172	0	0.002255
33	Seismic	LinModHist	Max	12.737022	0	0.002074
34	Seismic	LinModHist	Max	12.083591	0	0.001832
35	Seismic	LinModHist	Max	10.682229	0	0.001546
36	Seismic	LinModHist	Max	9.167608	0	0.001373
37	Seismic	LinModHist	Max	9.103339	0	0.001194
38	Seismic	LinModHist	Max	7.93827	0	0.001028
39	Seismic	LinModHist	Max	7.111796	0	0.000845
40	Seismic	LinModHist	Max	5.645438	0	0.000648
41	Seismic	LinModHist	Max	4.114852	0	0.000439
44	Seismic	LinModHist	Max	2.437977	0	0.000222

TABLE: Joint Displacements_2960 tons						
Joint	OutputCase	CaseType	StepType	U1	U2	U3
Text	Text	Text	Text	m	m	m
3	Seismic	LinModHist	Max	12.546969	0	0.002248
32	Seismic	LinModHist	Max	12.394278	0	0.002205
33	Seismic	LinModHist	Max	12.402114	0	0.002028
34	Seismic	LinModHist	Max	11.773625	0	0.00179
35	Seismic	LinModHist	Max	10.416035	0	0.00151
36	Seismic	LinModHist	Max	8.982037	0	0.001341
37	Seismic	LinModHist	Max	9.0028	0	0.001166
38	Seismic	LinModHist	Max	7.881096	0	0.001004
39	Seismic	LinModHist	Max	7.073	0	0.000825
40	Seismic	LinModHist	Max	5.61313	0	0.000632
41	Seismic	LinModHist	Max	4.069113	0	0.000428
44	Seismic	LinModHist	Max	2.441046	0	0.000216

TABLE: Joint Displacements_7700 tons						
Joint	OutputCase	CaseType	StepType	U1	U2	U3
Text	Text	Text	Text	m	m	m
3	Seismic	LinModHist	Max	12.864988	0	0.002325
17	Seismic	LinModHist	Max	3.946716	0	0
32	Seismic	LinModHist	Max	12.709524	0	0.00228
33	Seismic	LinModHist	Max	12.693235	0	0.002097
34	Seismic	LinModHist	Max	12.057953	0	0.001852
35	Seismic	LinModHist	Max	10.695759	0	0.001563
36	Seismic	LinModHist	Max	9.250566	0	0.001388
37	Seismic	LinModHist	Max	9.249038	0	0.001207
38	Seismic	LinModHist	Max	8.093253	0	0.001039
39	Seismic	LinModHist	Max	7.244937	0	0.000854
40	Seismic	LinModHist	Max	5.74219	0	0.000655
41	Seismic	LinModHist	Max	4.150856	0	0.000444
44	Seismic	LinModHist	Max	2.486927	0	0.000224